Accepted to ApJ: 7 February, 2008. Reproduced with the permission of the AstroPhysical Journal
Preprint typeset using LaTeX style emulateapj v. 12/14/05

arXiv:0802.2549v1 [astro-ph] 18 Feb 2008

UNVEILING THE IMPORTANT ROLE OF GROUPS IN THE EVOLUTION OF MASSIVE GALAXIES: INSIGHTS FROM AN INFRARED PASSIVE SEQUENCE AT INTERMEDIATE REDSHIFT

D. J. Wilman[1], D. Pierini[1], K. Tyler[2], S. L. McGee[3], A. Oemler Jr[4], S. L. Morris[5], M. L. Balogh[3], R. G. Bower[5], J. S. Mulchaey[4]
[1]Max-Planck-Institut für extraterrestrische Physik, Giessenbachstraße, D-85748 Garching, Germany.
[2]Steward Observatory, University of Arizona, 933 North Cherry Avenue, Tucson, AZ 85721, U.S.A.
[3]Department of Physics and Astronomy, University of Waterloo, Waterloo, Ontario, N2L 3G1, Canada.
[4]Observatories of the Carnegie Institution, 813 Santa Barbara Street, Pasadena, California, U.S.A.
[5]Physics Department, University of Durham, South Road, Durham DH1 3LE, U.K.

Accepted to ApJ: *7 February, 2008. Reproduced with the permission of the AstroPhysical Journal*

ABSTRACT

The most massive galaxies in the Universe are also the oldest. To overturn this apparent contradiction with hierarchical growth models, we focus on the group-scale haloes which host most of these galaxies. Our $z \sim 0.4$ group sample is selected in redshift space from the CNOC2 redshift survey. A stellar mass selected $\mathrm{M}_* \gtrsim 2 \times 10^{10}\,\mathrm{M}_\odot$ sample is constructed using IRAC observations. A sensitive Mid InfraRed (MIR) IRAC colour is used to isolate passive galaxies. It produces a bimodal distribution, in which passive galaxies (highlighted by morphological early-types) define a tight MIR colour sequence (Infrared Passive Sequence, IPS). This is due to stellar atmospheric emission from old stellar populations. Significantly offset from the IPS are galaxies where reemission by dust boosts emission at λ_{obs}=8μm. We term them InfraRed-Excess galaxies whether star formation and/or AGN activity are present. They include all known morphological late-types. Comparison with EW[OII] shows that MIR colour is highly sensitive to low levels of activity, and allows us to separate dusty-active from passive galaxies at high stellar mass. The fraction of InfraRed Excess galaxies, f(IRE) drops with M_*, such that f(IRE) = 0.5 at a "crossover mass" of $\mathrm{M}_{\mathrm{cr}} \sim 1.3 \times 10^{11}\,\mathrm{M}_\odot$. Within our optically-defined group sample there is a strong and consistent deficit in f(IRE) at all masses, but most clearly at $\mathrm{M}_* \gtrsim 10^{11}\,\mathrm{M}_\odot$. Suppression of star formation must mainly occur in groups. In particular, the observed trend of f(IRE) with M_* can be explained if suppression of $\mathrm{M}_* \gtrsim 10^{11}\,\mathrm{M}_\odot$ galaxies occurs primarily in the group environment. This is confirmed using a mock galaxy catalogue derived from the Millenium Simulation. In this way, the mass-dependent evolution in f(IRE) (*downsizing*) can be driven solely by structure growth in the Universe, as more galaxies are accreted into group-sized haloes with cosmic time.

Subject headings: galaxies: statistics — galaxies: evolution — infrared: galaxies — galaxies: photometry — galaxies: high-redshift — galaxies: clusters: general

1. INTRODUCTION

Perhaps the biggest puzzle of galaxy formation in recent decades has been the early and rapid formation of the most massive galaxies (Bender et al. 1998; Cimatti et al. 2004). This apparently supported the "monolithic collapse" model (Eggen et al. 1962), in contradiction to the standard picture of a Cold Dark Matter (CDM) Universe, in which galaxies grow hierarchically through mergers, along with the dark matter haloes in which they are embedded (e.g. Benson et al. 2002). Observationally, the picture has been embellished by recent galaxy surveys from $z \sim 0$ to $z \sim 1.5$. Going to higher galaxy mass and to denser environments, galaxies are older (Kauffmann et al. 2003; Panter et al. 2003; Poggianti et al. 2004; Thomas et al. 2005; Salim et al. 2005) and more likely to have experienced a shorter star forming life which is now truncated (Yamada et al. 2005; Baldry et al. 2006; Pannella et al. 2006; Haines et al. 2007; Bundy et al. 2006; Hopkins et al. 2007). The term *downsizing* (Cowie et al. 1999) is used to describe the earlier and less extended star formation histories in more massive galaxies.

Recent attempts to explain downsizing trends have examined the ways in which gas heating and cooling depend upon mass and redshift (e.g. Dekel & Birnboim 2006), and invoked new heating methods such as feedback from Active Galactic Nuclei (AGN, Bower et al. 2006; Croton et al. 2006). Regardless of the physics, a hierarchical Universe can itself supply a natural explanation for dependence of galaxy properties upon stellar mass and upon environment at the same time (De Lucia et al. 2006). As more and more massive galaxies are encorporated into more and more massive haloes, the probability of star formation being truncated is increased. Even in the populous loose group environment the properties of galaxies depend strongly upon environment (e.g. Postman & Geller 1984; Zabludoff & Mulchaey 1998; Lewis et al. 2002; Gómez et al. 2003; Balogh et al. 2004; Wilman et al. 2005; Weinmann et al. 2006; Gerke et al. 2007). Thus, evolution in groups can play an important role in driving evolutionary trends.

The fraction of passive galaxies increases steadily and monotonically with increasing stellar mass. It is therefore convenient to quantify downsizing trends by identifying a stellar mass at which the fraction of passive (or red/early-type) galaxies is defined to be exactly 50%. This has no physical significance, and so we prefer to call this the "*crossover mass*" (M_{cr}) rather than the "*transition mass*" (e.g. Bundy et al. 2006). $\mathrm{M_{cr}}$ decreases strongly with increasing environmental density (Baldry et al. 2006; Bundy et al. 2006; Haines et al. 2007), with a maximum $\mathrm{M_{cr}} \sim 2\times10^{10}\,\mathrm{M_\odot}$ in the *lowest density environments* where the $z \sim 0$ red galaxy fraction is 50% (Baldry et al. 2006). The evolution of $\mathrm{M_{cr}}$ for the global population, indicates $\mathrm{M_{cr}} \sim 2.5 - 6 \times 10^{10}\,\mathrm{M_\odot}$ at $z \sim 0.4$ and $\mathrm{M_{cr}} \sim 7 - 10 \times 10^{10}\,\mathrm{M_\odot}$ at $z \sim 1$ (Hopkins et al. 2007).

These studies, mostly at rest-frame UV to optical wavelengths, are hindered by the strong correlation between galaxy mass and dust attenuation in star-forming galaxies (Giovanelli et al. 1995; Wang & Heckman 1996; Masters et al. 2003; Brinchmann et al. 2004; Weiner et al. 2007). This correlation may arise directly from the variations of star formation history with mass (Calura et al. 2007) and can lead to confusion between truly passive and dusty star forming galaxies. In some cases light from the youngest stars can be totally removed from the line of sight, not only because their SED peaks at shorter wavelengths where dust attenuation is most effective (e.g. Pierini et al. 2004), but also because the HII regions in which they are embedded can be particularly dusty (Duc et al. 2002; Tuffs et al. 2004). This degeneracy of passive versus dusty star forming galaxies is well known at high redshifts, where a selection of optically red galaxies (Extremely Red Object/Galaxy -ERO/ERG or Distant Red Galaxy - DRG) is more and more likely to select dusty starbursts as one moves to even higher redshift (from $\sim 50\%$ at $z \sim 1$ (Cimatti et al. 2002; Lotz et al. 2008) to $\gtrsim 90\%$ at $z \sim 2-3$ (Papovich et al. 2006), with an increasing contribution from increasingly active infrared-bright galaxies (Caputi et al. 2006; Daddi et al. 2007)).

Even in the local Universe the optical red sequence (e.g. Bower et al. 1992) is contaminated with star-forming galaxies and some AGN. These "interlopers" can be identified using optical or UV colour-colour diagrams or high signal to noise emission line measurements (e.g. Wolf et al. 2005; Haines et al. 2007). However the dust emission really stands out in the infrared where the absorbed energy (mainly non-ionizing UV photons) is re-emitted (Popescu et al. 2000, and references therein). 31% of red-sequence galaxies (by number density) are 24μm-bright, corresponding to $\sim$ 17% star-forming galaxies and $\sim$ 14% AGN-host galaxies (Davoodi et al. 2006).

At shorter wavelengths ($\sim$3-12μm) strong emission features exist in the presence of star formation (Phillips et al. 1984; Roche et al. 1991). However they are usually absent in the more highly ionized environments typical of AGN (Aitken et al. 1982; Roche et al. 1984, 1991). These have been identified as PAH (Polycyclic-Aromatic-Hydrocarbon) features (most obviously characterized by the strong, broad emission features at 6.2μm 7.7μm 8.6μm and 11.3μm, Leger & Puget 1984; Desert et al. 1990), and loosely trace star formation rates on the scale of a galaxy (Roussel et al. 2001). Spectral diagnostics have been developed using the strengths of these features to distinguish star formation from nuclear activity (Genzel et al. 1998; Laurent et al. 2000). PAH carriers are apparently ubiquitous in high metallicity star-forming galaxies (e.g. Boselli et al. 1998; Genzel & Cesarsky 2000; Draine et al. 2007), although in low metallicity galaxies they may be absent (Engelbracht et al. 2005; Draine et al. 2007). Calibration of physical quantities, such as star formation rate, from PAH bands is complicated by the relative importance of circumstellar dust, and diffuse dust heated by the general radiation field or collisional impacts. These components may be significant for galaxies with low to moderate star formation rates and dust contents (see e.g. Boselli et al. 2004; Pérez-González et al. 2006; Calzetti et al. 2007).

To keep things simple, one can construct Mid-InfraRed (MIR) colours as opposed to calibrating star formation rates. The wealth of information in this spectral range prompted the use of MIR colours to trace star formation, dust temperature and nuclear activity (e.g. Dale et al. 2000; Boselli et al. 2003; Fisher 2006). Normalizing the flux from a dust-sensitive band ($\lambda_{\rm rest} \gtrsim 6\mu$m) by a stellar mass-sensitive band (tracing old stellar populations, e.g. at 3.6μm) produces a MIR colour highly sensitive to the level of dust emission per unit stellar mass. This is especially well correlated with morphology, tracing the warm dust emission from star-forming spiral arms (Pahre et al. 2004a). Indeed, in the local Universe, the MIR colour can effectively predict morphology. Li et al. (2007) find 88% early-types below $\nu\mathrm{L}_\nu(8)/\nu\mathrm{L}_\nu(3.6) = 0.303$ and 83% late-types above this division [1]. The combined sample exhibits a bimodal distribution in MIR colour. Johnson et al. (2007) also see this bimodality in MIR colours for galaxies in Hickson Compact Groups, and show that the fraction of MIR-passive galaxies is much higher in the more evolved (HI-poor and X-ray bright) groups. These results demonstrate the power of IRAC colours to separate truly passive galaxies from star-forming or AGN-host galaxies without the dust-driven degeneracies of optical and UV studies.

Our goal is to isolate truly passive galaxies and thus trace the build-up of the increasingly important population of passively evolving galaxies in the Universe, as a function of environment. In particular, we wish to study massive ($\mathrm{M_*} \gtrsim 2\times10^{10}\,\mathrm{M_\odot}$) galaxies at $z \sim 0.4$, where the contributions of both passive and dusty star-forming galaxies are important, but can be confused with each other without due attention. Separating these populations using the MIR colour will alleviate this problem. Strong evolution in the dust and star formation properties of normal galaxies over the range $0 < z \lesssim 0.7$ is expected: At $z \gtrsim 0.7$ spirals dominate the Luminous InfraRed Galaxy (LIRG) population (Bell et al. 2005; Rowan-Robinson et al. 2005; Zheng et al. 2007), whilst today galaxies of equivalent infrared luminosities are much rarer, and are typically interacting systems and mergers. Our galaxy sample, selected from the CNOC2 redshift survey (Yee et al. 2000), probes intermediate redshifts ($z \sim 0.4$). This redshift corresponds to a look-back time of $\sim 3-4$ Gyr, when the volume-averaged star formation rate in the Universe was significantly higher than it is today (Lilly et al. 1996; Madau et al. 1998; Hopkins 2004).

In Section 2 our sample is introduced, including archive IRAC data in our fields. From this stellar masses and

---

[1] Includes assumed stellar contribution to $\nu\mathrm{L}_\nu(8)$ of $0.232\nu\mathrm{L}_\nu(3.6)$.

MIR colours are derived, a mass-selected sample is constructed. Selection effects will be discussed in detail. Section 3 presents the MIR colours of $z \sim 0.4$ galaxies as a function of their stellar masses and morphologies. A tight *Infrared Passive Sequence* is identified in the MIR colour-mass plane as a tool to select passive galaxies. Section 4 examines the correlation of MIR colour with the EW[OII]λ3727 emission line diagnostic, testing their relative sensitivity. In Section 5 we compute the fraction of massive galaxies with InfraRed Excess (IRE galaxies) as a function of stellar mass. The role of the group environment is discussed in Section 6, where we examine galaxies in our optical group catalogue (Carlberg et al. 2001). Finally, our results are discussed in the context of our current understanding of galaxy evolution and the group environment in Section 7. In particular, by applying a simple model to a mock galaxy catalogue, we focus on the possibility that downsizing is intimately related to, if not entirely caused by, the growth of structure with time. Our conclusions are presented in Section 8. Throughout this paper a ΛCDM cosmology with $\Omega_{\rm m} = 0.3$, $\Omega_\Lambda = 0.7$ and $H_0 = 100h\,{\rm km\,s^{-1}\,Mpc^{-1}}$ with h=0.75 is assumed.

2. SAMPLE

The objective of this paper is to study MIR activity in galaxies as a function of their stellar mass and environment. This is facilitated by the construction of a mass-selected sample in the redshift range $0.3 \leq z \leq 0.48$, described in this section.

2.1. *CNOC2 Survey and Groups*

Our sample is based upon the CNOC2 redshift survey which is magnitude limited down to $R_C \sim 23.2$ in photometry and totals $\sim 1.5\Box^\circ$ within four separate patches on the sky. Spectroscopic redshifts exist for a large and unbiased sample of $R_C \lesssim 21.5$ galaxies (Yee et al. 2000). Within the fields of 20 kinematically selected groups from the catalogue of Carlberg et al. (2001), the original $UBVR_CI_C$ photometry and spectroscopy have been supplemented with targetted spectroscopy to $R_C = 22$ using the Magellan 6.5m telescope (Wilman et al. 2005), and F775W-band HST ACS imaging. Galaxies with spectroscopic redshifts $z > 0.3$ and ACS coverage have been visually morphologically classified by one of the authors (Augustus Oemler Jr, hereafter AO).

The probability that a galaxy has a redshift is a function of its R_C-band magnitude, and is unbiased to $R_C = 21.5$. To study the statistical properties of galaxies as a function of their stellar mass (and not R_C-band magnitude), we must statistically correct for this selection function and magnitude limit. This is achieved by weighting galaxies by the inverse probability that they appear in the $R_C \leq 21.5$ spectroscopic sample. There are two components to this weight:

- A weight W_{R_C} to account for the fraction of galaxies which are targetted spectroscopically (with measured redshifts) as a function of R_C-band magnitude. Since below $R_C = 21.5$ the success of redshift determination may be biased in favour of emission line galaxies, W_{R_C} is set to 0 for $R_C > 21.5$.
- A weight W_z to account for the fraction of sample volume within which a galaxy would fall out of our $R_C \leq 21.5$ sample (effectively a $V_{\rm max}$ correction). For a $0.3 \leq z \leq 0.48$ sample, this means that for each $R_C \leq 21.5$ galaxy in the sample, $W_z = V(z = 0.3 \text{ to } z = 0.48)/V(z = 0.3 \text{ to } z = z_{\rm lim})$ where V is the cosmological volume in our chosen cosmology, and $z_{\rm lim}$ is the redshift at which the galaxy would have a magnitude $R_C = 21.5$.

Then the final weight for each galaxy is simply: $W = W_{R_C} \times W_z$.

2.2. *IRAC Photometry*

The *Spitzer Space Telescope* GTO program 64 (PI Fazio) included an IRAC (Infrared Array Camera, Fazio et al. 2004) scan-map survey of $\sim 20' \times 30'$ regions in the centre of three of the four CNOC2 patches. The IRAC focal plane geometry translates each mapping into one mapping of bands 1 (3.6μm) and 3 (5.8μm) and another mapping of bands 2 (4.5μm) and 4 (8.0μm), offset by 6.7′.

The astrometrically and photometrically calibrated post-BCD (Post – Basic Calibrated Data) products were retrieved from the Spitzer archive. The pipeline version used was S11.4.0. The processed images are clean, with no image artifacts, and provide stable source flux measurements and accurate sub-arcsecond astrometry. Apart from at the map edges, all sources receive ~500 s imaging time in all four bands (100 s frame-time at five dithered positions). The complete four band IRAC coverage has significant ($\geq 50\%$) overlap with six ACS fields, where galaxies have also been morphologically classified. Shallow MIPS 24μm imaging is also available, but with lower sensitivity and poorer diffraction-limited resolution than the IRAC bands.

For all sources detected in the 3.6μm frame, colours are measured using the *SExtractor* package (Bertin & Arnouts 1996) in *double-image* mode. They are derived from fluxes measured inside 3″ radius apertures centred at the position of all 3.6μm detected objects, in all IRAC bands. Detection requires at least four adjacent pixels which are at least 1.5-σ above the background level at 3.6μm. Aperture corrections were computed to correct for light lost from the aperture due to the spatial extent of the PRF (Point Response Function)[2]. Corrected measurements are used to compute flux ratios (colours) within the aperture. The *SExtractor* FLUX_AUTO Kron-like measurement provides more stable total flux measurements, and thus is used to compute absolute galaxy luminosity at 3.6μm. We follow the practice of SWIRE[3] and compute the flux error from the measurement image itself, weighted by inverse variance using the coverage map.

To match the 3.6μm selected catalogue to the CNOC2 redshift catalogue, we apply the *tmatch* tool in *iraf* [4].

---

[2] Measured by combining larger aperture measurements for isolated stars with IRAC Data Handbook values. Corrections are 1.184, 1.180, 1.249 and 1.404 for IRAC bands 1-4 respectively.

[3] swire.ipac.caltech.edu/swire/astronomers/publications

[4] IRAF is distributed by the National Optical Astronomy Observatories, which are operated by the Association of Universities for Research in Astronomy, Inc., under cooperative agreement with the National Science Foundation

None of the galaxies in our spectroscopic sample are lost from the IRAC sample due to lack of sensitivity except at the edge of the IRAC field. Visual inspection shows that CNOC2 galaxies with no match either lie outside the IRAC zone of full coverage, can be identified with sources improperly deblended by *SExtractor*, or lie in regions of particularly poor CNOC2 astrometry. The sample is then limited to those objects with unambiguous matches, with no apparent bias relative to the $\sim 15\%$ of CNOC2 galaxies with IRAC coverage which are lost at this stage. However, to maintain statistical accuracy the weight $\mathrm{W}_{\mathrm{R_C}}$ is modified to account for galaxies without spectroscopy or 3.6μm matches, as a function of $\mathrm{R_C}$-band magnitude. At 3.6μm, the 2-σ depth is $\sim$1μJy (for a passive galaxy at z=0.4, this corresponds to a stellar mass of $\sim 9 \times 10^8\,\mathrm{M}_\odot$).

The goal is to construct a $0.3 \leq z \leq 0.48$ mass-selected sample for which representative spectroscopy is available, and reaching required depth at 8μm to distinguish passive galaxies from those with excess emission at 8μm (2-σ depth of $\sim$10μJy). Effectively, these criteria set the mass limit to $2 \times 10^{10}\,\mathrm{M}_\odot$, well above the 3.6$\mu$m limit (§ 2.4 for more details).

2.3. *Deriving Stellar Masses and MIR Colours*

2.3.1. *Stellar Mass*

Near InfraRed (NIR) light is a useful tracer of stellar mass because of the weak dependence on star formation history (Aaronson et al. 1979; Rix & Rieke 1993; Bell & de Jong 2001). 3.6μm flux has been converted into luminosity and thence to stellar mass following Balogh et al. (2007). To give a brief overview of this procedure: Observed-frame AB luminosities are computed for the assumed cosmology, and an empirical k-correction is applied to correct to a consistent rest-frame of a $z = 0.4$ galaxy. In this paper, we will call this $^{0.4}[3.6]$. Secondary corrections are then applied to move into the K-band rest-frame. These corrections are calibrated for objects with both [3.6] and K-band photometry (not used in this paper). The mass to light ratio of each galaxy in K-band ($\mathrm{M}_*/\mathrm{L_K}$) is estimated using a combination of two simple Bruzual & Charlot (2003) models with a Chabrier (2003) IMF. For blue galaxies ($\mathrm{B} - \mathrm{V} < 0.4$), a constant star formation model with dust extinction τ_v =1 mag gives $\mathrm{M}_*/\mathrm{L_K} = 0.2$. For red galaxies ($\mathrm{B} - \mathrm{V} > 1.0$), a 11.7-Gyr old, dust free single stellar population model gives $\mathrm{M}_*/\mathrm{L_K} = 0.7$. For intermediate colours a linear interpolation between these values is used. For more details, please refer to Balogh et al. (2007). This means that the full range of galaxy types only exhibit a range in $\mathrm{M}_*/\mathrm{L_K}$ (and thus also $\mathrm{M}_*/\mathrm{L}_{^{0.4}[3.6]}$) of 3.5. Therefore our results are relatively insensitive to whether we select in mass or $^{0.4}[3.6]$ luminosity. We prefer to select in mass as it is the more physical quantity and, thus, allows a comparison with the literature.

2.3.2. *MIR colour*

The two template spectra in the top panel of Figure 1 demonstrate the diversity and wealth of spectral information at MIR wavelengths. A passive, dust-free galaxy is likely to exhibit a spectrum similar to the SSP template (dashed line). With no dust emission, the infrared emission originates solely from photospheres of the cold stellar population, primarily giant M-stars. Conversely, the spectrum of a dusty star forming galaxy should look more like that of M82 (solid line). Beyond $\lambda_{\mathrm{rest}} \sim 3 - 4\mu$m, a typical dust emission spectrum with characteristic PAH features comes to dominate the M82 template.

The lower panel of Figure 1 shows the transmission function of the IRAC bands at 3.6μm and 8μm, and the MIPS (Multi-Band Imaging Photometer for Spitzer, Rieke et al. 2004) 24μm band. Each transmission function is transformed to indicate the rest-frame wavelength domain probed for a galaxy located at $z = 0.3$,0.4 or 0.5. It is clear that excess (enhanced beyond pure stellar photospheric) emission can be revealed at both 8μm and 24μm for galaxies within the redshift range of interest. For $0.05 \lesssim z \lesssim 0.48$ galaxies, the 8μm band captures the strong 6.2μm PAH feature, tracing star formation (e.g. Peeters et al. 2004; Förster Schreiber et al. 2004). Crucially, stellar atmospheric emission drops off significantly from 8μm to 24μm: Thus detection of passive galaxies, and thence accurate separation of passive from star-forming or AGN-host galaxies, requires much shallower exposures at 8μm than 24μm. A colour constructed from 8μm and 3.6μm has the leverage on the galaxy spectrum to make this distinction. In this paper we focus on IRAC data for these reasons.

For the sake of simplicity, we compute k-corrected MIR colours of our galaxies using a linear combination of the two simple templates in Figure 1 (similar to the approach of Huang et al. 2007). We define our colour to be the flux-ratio $[\mathrm{f}(8)/\,\mathrm{f}(3.6)]$ [5]. For each galaxy, the quantity η is measured: This is the required fractional contribution from the M82 template to match the *observed-frame* $^{\mathrm{z}}[\mathrm{f}(8)/\,\mathrm{f}(3.6)]$ [6]. Our k-corrections are based on the assumption that η (approximately *dust to stellar flux ratio*), would be the same regardless of the redshift of the galaxy (and thus the part of the spectrum sampled). η is computed as:

$$\eta = \frac{^{\mathrm{z}}[\mathrm{f}(8)/\,\mathrm{f}(3.6)] - {}^{\mathrm{z}}[\mathrm{f}(8)/\,\mathrm{f}(3.6)](\mathrm{SSP})}{^{\mathrm{z}}[\mathrm{f}(8)/\,\mathrm{f}(3.6)](\mathrm{M82}) - {}^{\mathrm{z}}[\mathrm{f}(8)/\,\mathrm{f}(3.6)](\mathrm{SSP})} \tag{1}$$

To minimize the k-corrections $^{\mathrm{z}}[\mathrm{f}(8)/\,\mathrm{f}(3.6)]$ is transformed to the equivalent colour for a z=0.4 galaxy, and limit ourselves to galaxies in the narrow redshift range $0.3 \leq z \leq 0.48$, an epoch $\gtrsim 3\,\mathrm{Gyr}$ ago. The k-corrected $[\mathrm{f}(8)/\,\mathrm{f}(3.6)]$ colour is computed as:

$$^{0.4}[\mathrm{f}(8)/\,\mathrm{f}(3.6)] = \eta \times {}^{0.4}[\mathrm{f}(8)/\,\mathrm{f}(3.6)](\mathrm{M82}) + (1-\eta) \times {}^{0.4}[\mathrm{f}(8)/\,\mathrm{f}(3.6)](\mathrm{S} \tag{2}$$

A pure SSP k-correction ($< 0.07\,^{\mathrm{z}}[\mathrm{f}(8)/\,\mathrm{f}(3.6)]$) increases by $\lesssim 10\%$ going from ages of $8\,\mathrm{Gyr}$ to $1\,\mathrm{Gyr}$, and $10 - 20\%$ going from solar to 3× solar metallicity. For $\eta = 1$ (M82-like), $^{0.4}[\mathrm{f}(8)/\,\mathrm{f}(3.6)]$=2.17 ($\sim$ 7 times the stellar photospheric continuum emission within the IRAC 8μm band). Whilst k-corrections of high η galaxies are more uncertain due to the assumed M82 template, k-corrections remain relatively small within our redshift range ($\lesssim 50\%$ for $\eta = 1$). In this paper we will only sepa-

---

[5] for a more traditional colour, simply compute [3.6]-[8] = $+2.5\log_{10}([\mathrm{f}(8)/\,\mathrm{f}(3.6)])$

[6] The prefix superscipt z is used to indicate the band-pass (Blanton & Roweis 2007); i.e. the redshift of a galaxy for which the k-correction is defined to be zero.

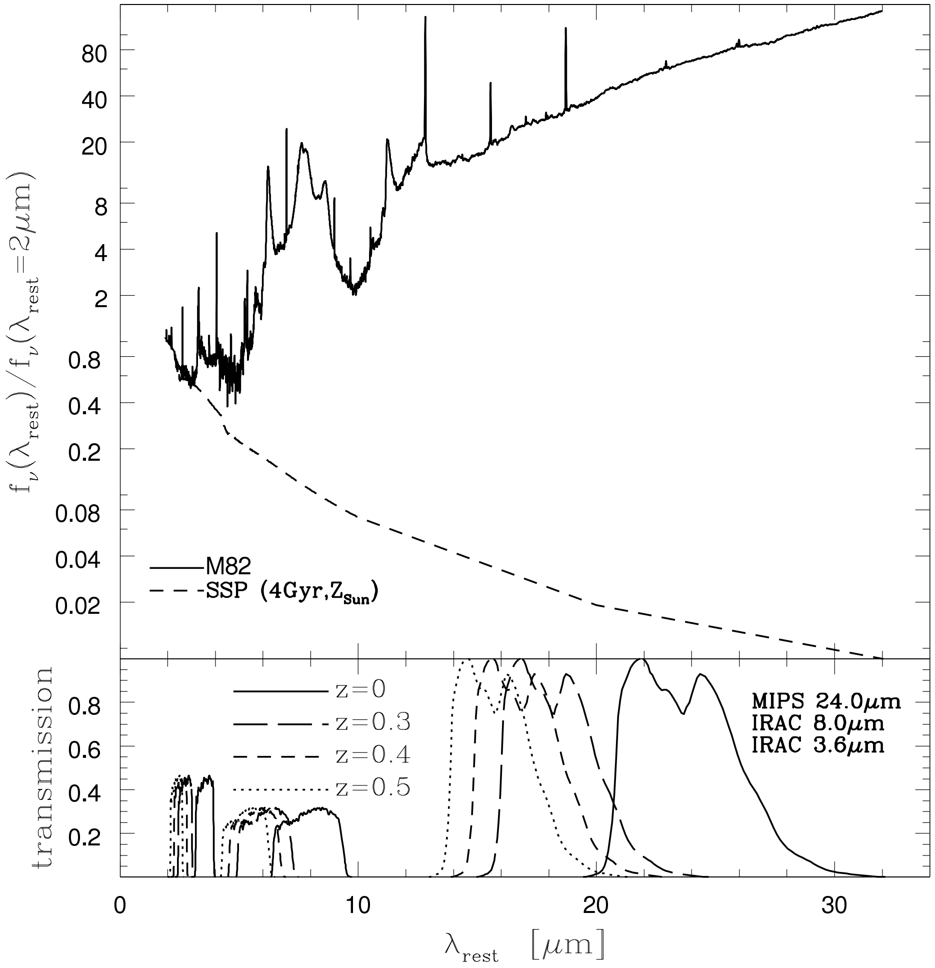

FIG. 1.— Our two MIR spectral templates are illustrated in the **top panel**. A 4 Gyr old Simple Stellar Population traces pure stellar atmospheric emission from old stars (SSP, dashed line). This is generated using *PEGASE2* (Fioc & Rocca-Volmerange 1997), with solar metallicity, and a Salpeter (1955) IMF with upper mass limit of 120 $M_\odot$. The other template is the ISO-SWS spectrum of the dusty star forming galaxy M82 (solid line, Förster Schreiber et al. 2001). The data is limited to $\lambda \geq 2.4\mu$m, and so we extrapolate down to 1.9μm by combining it with the spectrum obtained from a composite stellar population model (constant star formation rate, evolving metallicity, 1 Gyr since start of star formation, Salpeter IMF with upper mass limit of 120 $M_\odot$). The two templates are normalized to match at $\lambda = 2.2\mu$m. Beyond $\sim 3\mu$m, the spectrum of M82 is dominated by dust emission in the form of PAH features ($\lesssim 12\mu$m) and a warm dust emission continuum ($\gtrsim 12\mu$m). The **bottom panel** shows the effective transmission functions of Spitzer IRAC bands at 3.6μm and 8μm, and the MIPS 24μm band in the *rest-frames* of galaxies at $z = 0$ (solid), and $z = 0.3$ (long-dashed),0.4 (short-dashed) and 0.5 (dotted), corresponding to the redshift range of our galaxies. Whilst 3.6μm traces stellar emission, 8μm and 24μm trace PAH and warm dust emission respectively at $z \sim 0.4$.

rate dusty galaxies emitting excess light at infrared wavelengths from passive galaxies, and will not draw strong conclusions from precise MIR colours of dusty galaxies which are sensitive to the applied k-correction. To this extent, we believe that we are justified in applying these rough k-corrections.

2.4. *A Mass-Selected Sample*

In this paper, our analysis is limited to the subsample of galaxies with known redshifts $0.3 \leq z \leq 0.48$, and with full IRAC coverage. Of these, the 333 galaxies with stellar masses $M_* > 2\times10^{10} M_\odot$ are selected, corresponding to a luminosity of $^{0.4}$[3.6]=-20.89 for passively evolving galaxies, or a flux of f(3.6μm) > 20μJy, well above the detection limit.

This stellar mass limit is actually defined by the depth of the 8μm data, since we require this colour information for our analysis. In our mass-limited sample, 313 of the 333 galaxies are detected (2σ) at 8μm, and the remainder have $> 1.8\sigma$ upper limits that are sufficient to identify them as passively evolving galaxies, characterised by colours $^{0.4}[f(8)/f(3.6)] < 0.5$ (see § 3 for a justification of this definition).

The requirement that all galaxies have a spectroscopic redshift introduces sensitivity to the optical (R_C) selection function. To account for selection bias, the spectroscopic selection weight W is applied (§2.1). This weight includes the factor W_z which applies a volume correction to correct for galaxies which fall out of the $R_C \leq 21.5$ sample at $z_{\rm lim} \leq 0.48$. Within a $M_* \geq 2\times10^{10} M_\odot$ sample, the lowest mass and highest redshift galaxies with high mass to light ratios will not make this magnitude cut. Nonetheless, the weighted sample is still representative: A passively evolving $M_* = 2\times10^{10} M_\odot$ galaxy can be sampled with $R_C \leq 21.5$ up to a redshift of $z_{\rm lim} \sim 0.38$ ($\sim$ 36% of the volume sampled) and receives a weight $W_z = 1./0.36 = 2.78$. There do exist four $R_C \leq 21.5$ galaxies with unusually high mass to optical light ratios. These can more easily be lost from the sample due to their extremely red optical-NIR colours. Such red colours can exist where there is extreme dust extinction, or a population of AGB stars boosting NIR luminosity.

However, they are too few to significantly influence our statistics. Our sample of 333 galaxies includes eleven $M_* > 2 \times 10^{10}\,M_\odot$ galaxies with $R_C > 21.5$. These are assigned zero weight, but it is worth noting that the IRE fraction of these optically faint galaxies is comparable to that of other galaxies. In practice, our results are not strongly sensitive to the statistical weights.

3. BIMODAL MIR COLOURS AND A PASSIVE SEQUENCE

In this section the distribution of the MIR colour $^{0.4}[f(8)/f(3.6)]$, and its dependence on galaxy stellar mass M_* is investigated. Figure 2 shows how the 333 galaxies in our $M_* \geq 2{\times}10^{10}\,M_\odot$, $0.3 \leq z \leq 0.48$ sample populate the $^{0.4}[f(8)/f(3.6)]$- M_* "colour-mass" plane, along with the $25^{th}, 50^{th}$ and 75^{th} percentiles of the distribution.

The distribution shifts to lower $^{0.4}[f(8)/f(3.6)]$ with higher mass. Dust flux per unit stellar mass can be approximated by $^{0.4}[f(8)/f(3.6)]_{50\%} - 0.308$ where the stellar atmospheric contribution to $^{0.4}[f(8)/f(3.6)]$ is estimated by the SSP template to be $^{0.4}[f(8)/f(3.6)](SSP) = 0.308$ (dotted line). The median relation between $^{0.4}[f(8)/f(3.6)] - 0.308$ and stellar mass can be well fit by a linear relation in log space: $log_{10}(\,^{0.4}[f(8)/f(3.6)]_{50\%} - 0.308) = 8.8 \pm 0.2 - (0.85 \pm 0.02)\log_{10}(M_*/M_\odot)$. This relation is significantly shallower than would be expected for no relation between dust flux and stellar mass ($^{0.4}[f(8)/f(3.6)] - {}^{0.4}[f(8)/f(3.6)](SSP) \sim \frac{1}{M_*}$). However, this is sensitive to the exact value of $^{0.4}[f(8)/f(3.6)](SSP)$ chosen.

We also examine whether the strong correlation between MIR activity and morphology observed in the local Universe (Pahre et al. 2004a; Li et al. 2007) extends to our intermediate redshift sample. 31 of the galaxies in our sample are within the ACS fields and have been morphologically classified by AO. These are indicated in Figure 2.

Morphologically classified early-type (Elliptical and S0) and late-type (mainly spiral) galaxies exhibit very different MIR colour distributions, as seen locally by Li et al. (2007). In fact, the overall distribution in $^{0.4}[f(8)/f(3.6)]$ is bimodal in nature, with the two peaks in MIR colour almost equivalent to these two morphological classes. This bimodality has been observed in other (local) optical-NIR selected samples (Li et al. 2007; Johnson et al. 2007) whilst it is less obvious in shallow 8μm-selected samples where early-types are more difficult to detect (Huang et al. 2007). The bimodality of CNOC2 galaxies is demonstrated in Figure 3, split into two bins of stellar mass. Within each mass range there exists a significant population of galaxies with $^{0.4}[f(8)/f(3.6)] < 0.5$ and then a gap before the onset of a second population of galaxies emitting more strongly at 8μm. Whilst the full distribution seems to shift to higher $^{0.4}[f(8)/f(3.6)]$ at lower mass, the value $^{0.4}[f(8)/f(3.6)] = 0.5$ is within the gap across our mass range. Thus we adopt this value to divide the sample: Everything with $^{0.4}[f(8)/f(3.6)] > 0.5$ we call an **InfraRed-Excess (IRE)** galaxy. This division at 0.5 excludes galaxies from the passive population if they have 44% more 8μm flux than the early-type locus. Contribution from circumstellar dust (Piovan et al. 2003; Temi et al. 2008) or silicate emission from mass-loss (Bressan et al. 2007) are unlikely to produce such a strong boost to the 8μm flux.

The dash-filled histogram in Figure 3 indicates the $^{0.4}[f(8)/f(3.6)]$ distribution for morphologically early-type galaxies. The tight distribution of high mass early-types is mirrored in the narrow locus of almost constant colour in the colour-mass plane (Figure 2). The 11 early-types (ignoring the single upper limit) with $M_* > 6 \times 10^{10}\,M_\odot$ have mean colour and scatter $^{0.4}[f(8)/f(3.6)] \sim 0.347 \pm 0.03$ (horizontal dashed line in Figure 2). The scatter is consistent with the photometric errors. We call this the **Infrared Passive Sequence (IPS)**, which is not far offset from the template SSP colour ($^{0.4}[f(8)/f(3.6)] = 0.308$, horizontal dotted line). The peak value and scatter of the IPS for the full population of $M_* > 6 \times 10^{10}\,M_\odot$ galaxies is $^{0.4}[f(8)/f(3.6)] \sim 0.34 \pm 0.05$. The tight scatter of the IPS is reminiscent of the optical red sequence (e.g. Bower et al. 1992). Indeed the tightness of the IPS is due to the emission from stellar atmospheres of cold stars in passive galaxies, which is relatively little sensitivity to age or metallicity. Mid Infrared wavelengths are highly sensitive to dust emission; thus the Infrared Passive Sequence does not suffer from the degeneracy between dusty red galaxies and passive red galaxies as by a red sequence defined at optical wavelengths.

The second, broader peak at $^{0.4}[f(8)/f(3.6)] > 0.5$ contains IRE galaxies with excess (non-stellar) emission at 8μm. This excess emission traces some kind of activity, i.e. star formation or AGN. Figures 2 and 3 show that all known late-type galaxies (dot-filled histogram in Figure 3) in the sample inhabit this peak. Two morphologically classified early-type galaxies also exhibit excess emission at 8μm. Excess MIR emission in some early-type galaxies is known to exist, and correlates with low levels of star formation or AGN activity (e.g. Pahre et al. 2004b; Bressan et al. 2007).

4. THE $^{0.4}[f(8)/f(3.6)]$-EW[OII] PLANE

It is useful to compare the MIR colour $^{0.4}[f(8)/f(3.6)]$ with an independent, well-studied indicator of activity (primarily star formation), the equivalent width of the [OII]λ3727Å emission line. [OII] is most commonly used at z$\gtrsim$0.3 where the H$\alpha\lambda$6563Å emission line is redshifted out of the optical window. By normalizing the emission flux by the continuum level, the sensitivity to flux calibration and dust absorption is reduced, producing a normalized quantity more easily comparable to $^{0.4}[f(8)/f(3.6)]$.

Figure 4 shows the location of our $M_* \geq 2 \times 10^{10}\,M_\odot$ and $0.3 \leq z \leq 0.48$ galaxies (excluding 14 galaxies where EW[OII] could not be measured) in the $^{0.4}[f(8)/f(3.6)]$-EW[OII] plane, including 25^{th},50^{th} and 75^{th} percentiles and morphologically classified galaxies overplotted with their errors.

There is a strong correlation between EW[OII] and $^{0.4}[f(8)/f(3.6)]$. Both diagnostics trace galaxy activity, and primarily star formation, and so a strong correlation is expected. A value of EW[OII]= 2.1Å (dotted vertical line) corresponds to the median galaxy with $^{0.4}[f(8)/f(3.6)] = 0.5$ (our empirical division in MIR colour, solid horizontal line), which is below the [OII] detection limit of most spectroscopic surveys. Indeed, we are only able to identify this value for a large statistical sample: The median error on EW[OII] for individual

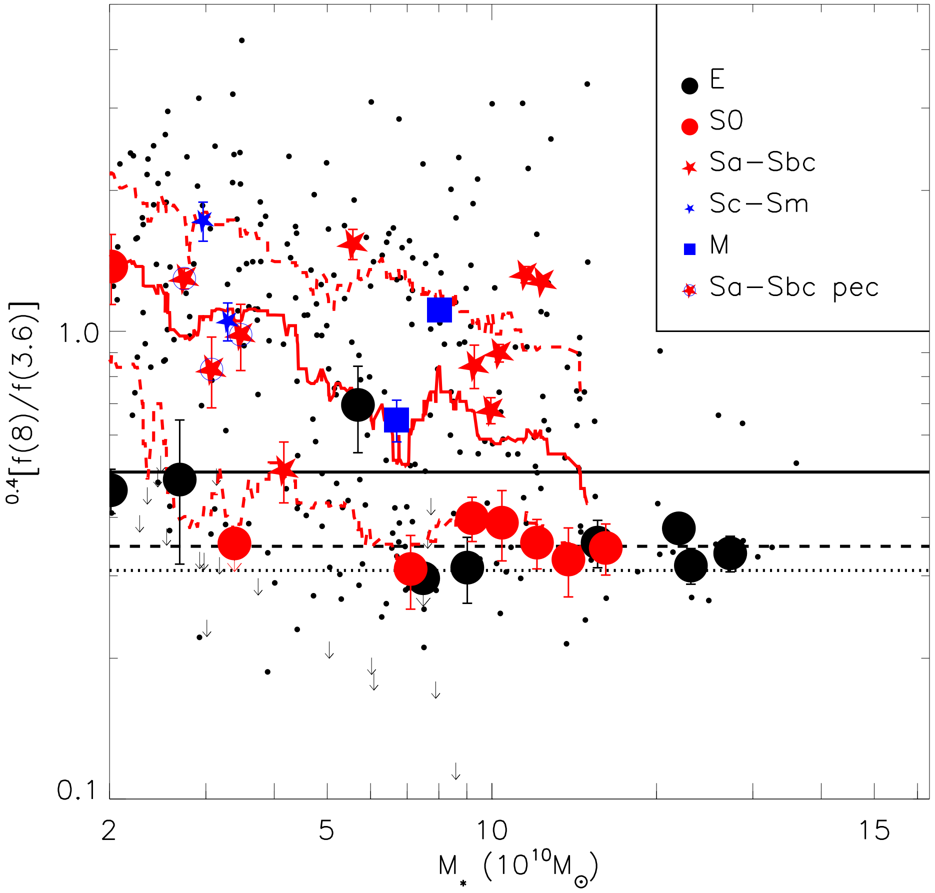

FIG. 2.— The $^{0.4}[f(8)/f(3.6)]$- M_* "colour-mass" plane for our sample of 333 $M_* \geq 2 \times 10^{10}\ M_\odot$, $0.3 \leq z \leq 0.48$ galaxies. For the few galaxies without 2σ 8μm detections, 2σ upper limits on $^{0.4}[f(8)/f(3.6)]$ are indicated. $25^{th}, 50^{th}$ and 75^{th} percentiles of the $^{0.4}[f(8)/f(3.6)]$ distribution are overplotted (red, solid and dashed lines). These are unweighted, and computed for running bins of 50 galaxies in M_*, and undetected galaxies are considered to be located at their measured values as opposed to upper limit values. Larger symbols are used for galaxies in the joint IRAC-ACS sample for which galaxies are morphologically classified (see key). For morphologically classified galaxies, measurement errors on $^{0.4}[f(8)/f(3.6)]$ are shown, which are typical of the overall population. Early-type galaxies cluster along a tight sequence at $^{0.4}[f(8)/f(3.6)] \sim 0.35$, consistent with pure stellar photospheric emission (horizontal dashed line). We call this the **Infrared Passive Sequence (IPS)**, and define InfraRed Excess (IRE) galaxies as those with $^{0.4}[f(8)/f(3.6)] > 0.5$ (horizontal solid line). The SSP template is indicated by the horizontal dotted line ($^{0.4}[f(8)/f(3.6)] = 0.308$).

galaxies in our sample is 2.4Å.

In Balogh et al. (2007), we divided our sample into passive and [OII]-strong galaxies at EW[OII]=10Å. This is the equivalent of a division at $^{0.4}[f(8)/f(3.6)] = 1.31$ for the median galaxy, selecting only the tail of galaxies with the most ongoing activity. A division at EW[OII]=5Å (as used in Wilman et al. 2005) corresponds to $^{0.4}[f(8)/f(3.6)] = 0.92$. Therefore with a reasonable photometric depth at $\lambda_{\rm rest} \sim 6\mu$m, it is possible to pick up levels of activity not possible without extremely deep optical spectroscopy. This inevitably leads to a higher fraction of galaxies defined as non-passive. Many spiral galaxies (mainly of type Sa-Sbc) with $^{0.4}[f(8)/f(3.6)] > 0.5$ have no detectable [OII] emission. Based upon a simple cut in EW[OII], these would be classified as passive spirals (e.g. Poggianti et al. 1999; Balogh et al. 2002). It is now clear that most such galaxies are not truly passive (in the sense of the IPS galaxies): instead there is evidence at 8μm of some ongoing activity. This indicates that the morphological transformation is more intimately linked to (and concurrent with) the complete cessation of star formation than previously believed.

The distribution of galaxies in the $^{0.4}[f(8)/f(3.6)]$-EW[OII] plane exhibits a lot of scatter around the median relation. Both EW[OII] and $^{0.4}[f(8)/f(3.6)]$ are highly sensitive to the presence of dust (through extinction of the [OII] emission by dust, and abundance of PAH carriers), which is itself dependent on the galaxy mass and star formation rate (Giovanelli et al. 1995; Wang & Heckman 1996; Masters et al. 2003; Brinchmann et al. 2004). Thus whilst MIR diagnostics are better at tracing activity in high mass galaxies, activity in lower mass galaxies may be better traced with optical diagnostics (especially at significantly sub-solar metallicity and thus very low mass where PAH features disappear, Engelbracht et al. 2005; Draine et al. 2007). However, within the mass range traced here, the median relation for EW[OII] goes as $\sim M_*^{-0.8}$, similar to the dependence of $^{0.4}[f(8)/f(3.6)]$ (once corrected for the stellar atmospheric contribution). To compute EW[OII], the [OII] line flux is normalized by the continuum at λ3727Å, which will lead to a shallower slope than would a normalizion by mass. It is likely that this effect counters any steeper relation expected due to different dust dependencies. Therefore, other physical parameters are necessary to drive the scatter in the $^{0.4}[f(8)/f(3.6)]$-EW[OII] plane, together with large measurement errors.

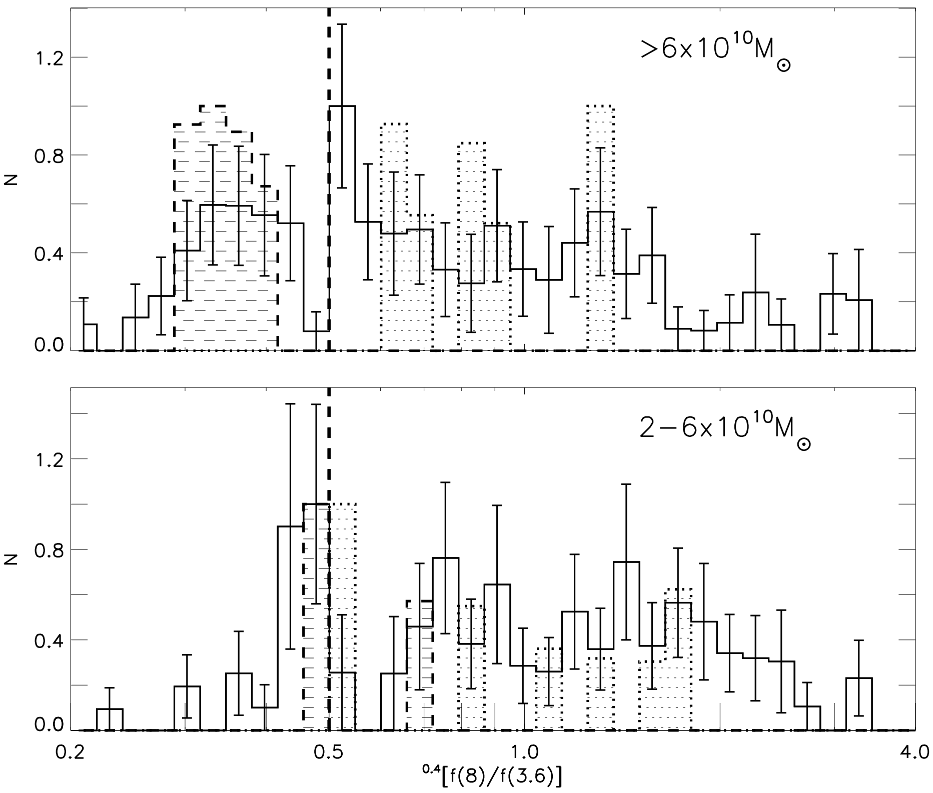

FIG. 3.— The weighted distribution of the MIR colour ${}^{0.4}$[f(8)/ f(3.6)] for $0.3 \leq z \leq 0.48$ galaxies with $\mathrm{M}_* > 6 \times 10^{10}\,\mathrm{M}_\odot$ **(top)** and $\mathrm{M}_* = 2 - 6 \times 10^{10}\,\mathrm{M}_\odot$ **(bottom)**, binned in log-space and with poissonian error-bars. The few galaxies without 2σ detections at 8μm are excluded. Since these are all constrained at the $\geq 1.8\sigma$ level to lie at ${}^{0.4}$[f(8)/ f(3.6)] < 0.5, their inclusion would not destroy the bimodality. Overplotted are the distributions for morphologically classified early type (dash-filled) and late type (dot-filled) galaxies, renormalized to give the same maximum value. Our criteria for an InfraRed Excess galaxy (${}^{0.4}$[f(8)/ f(3.6)] = 0.5) is indicated with the vertical dashed line, and effectively separates the peak of the **Infrared Passive Sequence (IPS)** (${}^{0.4}$[f(8)/ f(3.6)] < 0.5) from the InfraRed Excess (IRE) galaxy population.

There exists a strange population of galaxies extending to high EW[OII] at low ${}^{0.4}$[f(8)/ f(3.6)]. These galaxies diverge from the usual situation in massive galaxies: Namely, that infrared data traces activity to much lower levels than emission lines. For two of the four galaxies with ${}^{0.4}$[f(8)/ f(3.6)] ≤ 0.5 and EW[OII]> 20Å, the redshift depends upon a single emission line and might therefore be incorrect. Another possibility is that the [OII] emission originates in a low mass/metallicity galaxy which is falsely matched to a bright IRAC source. Visual checks suggest this is unlikely, but cannot be certain. Alternatively, these galaxies might be unusually bright at 3.6μm for their mass or metallicity. This may occur in metal-poor high mass galaxies (weird) or galaxies with a strong and very hot AGN component contributing most significantly to the 3.6μm-band (and AGN activity can also boost the [OII] emission, Yan et al. (2006)). The only morphologically classified galaxy at high EW[OII] and low ${}^{0.4}$[f(8)/ f(3.6)] is a merger galaxy. This could be explained by either of the above scenarios, or a third scenario in which a merger-driven starburst produces such a hard radiation field that it is capable of destroying the PAH carriers. Whatever their origin, these galaxies form a puzzling, possibly interesting, but small minority.

5. FREQUENCY OF INFRARED-EXCESS MASSIVE GALAXIES

Within our representative sample of $0.3 \leq z \leq 0.48$ and $\mathrm{M}_* \geq 2 \times 10^{10}\,\mathrm{M}_\odot$ galaxies, we now measure the fraction of **InfraRed Excess** galaxies, f(IRE).

Activity is traced with ${}^{0.4}$[f(8)/ f(3.6)] down to very low levels at which both star formation and nuclear activity play a role. We will not distinguish between these two forms of activity in this paper, instead merely computing the total fraction of IRE galaxies. However, any galaxy which has gas accreting onto a supermassive black hole is likely to be simultaneously forming stars (Brinchmann et al. 2004; Berta et al. 2007; Shi et al. 2007). Hence such galaxies are correctly distinguished from the passive population.

To measure f(IRE), the fraction of galaxies with ${}^{0.4}$[f(8)/ f(3.6)] > 0.5 is computed, with galaxies weighted to account for the magnitude-dependent selection function (Section 2.4). The application of this weight does not significantly change the results. To place errors on f(IRE), we perform bootstrap resampling of the sample. This is done by creating 1000 independent samples of the same size as the true sample: Within each sample, values of ${}^{0.4}$[f(8)/ f(3.6)] are taken randomly and often repeatedly from the true sample, and scattered using a gaussian kernel of width equal to the error on ${}^{0.4}$[f(8)/ f(3.6)]. The standard deviation of f(IRE) from the bootstrap samples is taken for the error on f(IRE).

Figure 5**(a)** (solid points and line) shows f(IRE) binned by stellar mass for the global population. Bins are not equally populated. Instead they are defined such that there is an approximately equal number of group galaxies per bin (§ 6). ${}^{0.4}$[f(8)/ f(3.6)] declines with M_*, an effect seen previously in the median and percentiles.

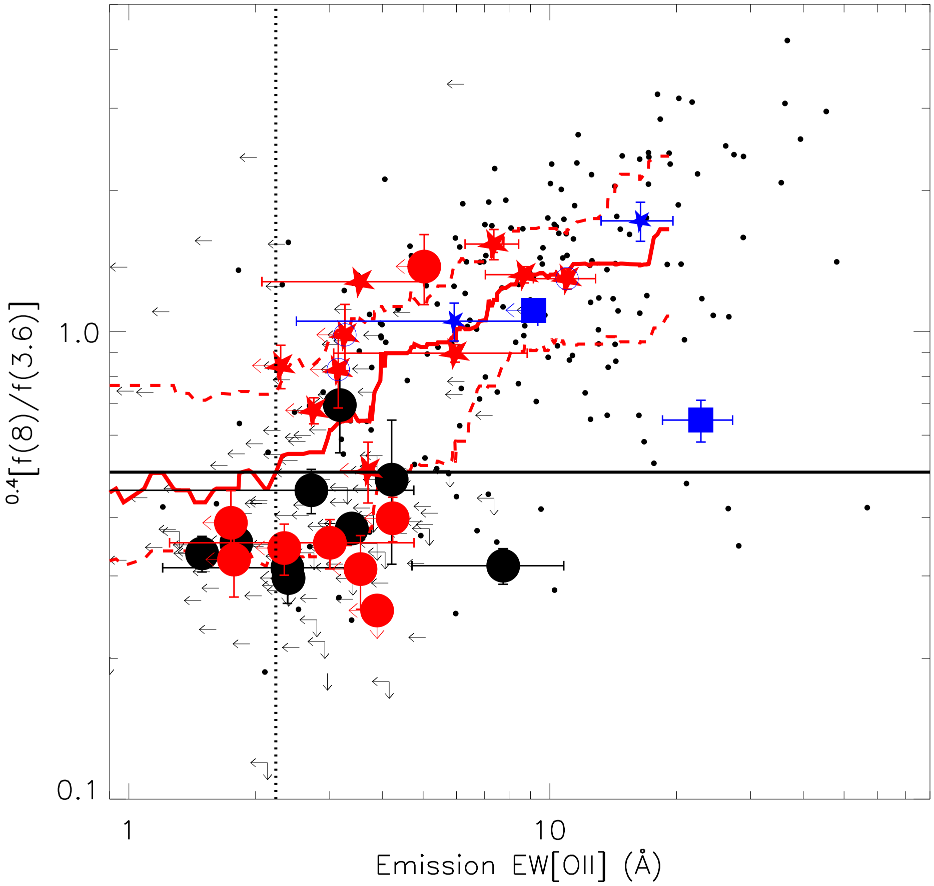

FIG. 4.— The $^{0.4}[f(8)/f(3.6)]$ - EW[OII] plane for 319 $M_* \geq 2 \times 10^{10} M_\odot$ and $0.3 \leq z \leq 0.48$ galaxies. $25^{th}, 50^{th}$ and 75^{th} percentiles of the $^{0.4}[f(8)/f(3.6)]$ distribution are overplotted, computed over running bins of 50 galaxies in EW[OII] (red, solid and dashed lines). Undetected galaxies (at the 1σ level in [OII] or the 2σ level at 8μm) are plotted at their 1σ EW[OII] and 2σ $^{0.4}[f(8)/f(3.6)]$ upper limit levels (arrows), whilst the percentiles are computed based upon *measured* [OII] and 8μm flux levels: on a statistical basis the 50^{th} percentile should therefore be representative of the true median relation (both measured [OII] and 8μm flux can be negative for non-detections). Our empirical division ($^{0.4}[f(8)/f(3.6)] = 0.5$) is overplotted (solid horizontal line). There is a strong correlation between EW[OII] and $^{0.4}[f(8)/f(3.6)]$, inferring that for the average galaxy both diagnostics trace the same phenomenon (primarily star formation). The median galaxy at our empirical division $^{0.4}[f(8)/f(3.6)] = 0.5$ has EW[OII]= 2.1Å (dotted vertical line). Larger symbols are used for morphologically classified galaxies as in Figure 2, with measurement errors typical of the overall population.

However this is only evident in the highest mass bin.

To test for effects of cosmic variance, this exercise is repeated independently for each of the three CNOC2 patches with IRAC coverage [7]. The patch to patch offsets in f(IRE) are $\lesssim 3\%$, compatible with the bootstrap errors, and indicating that cosmic variance is not a dominant source of error. Therefore this result is robust.

The *crossover mass* (M_{cr}, where f(IRE) = 0.5: dotted horizontal line), is $M_{cr} \sim 1.3 \times 10^{11} M_\odot$ (dashed vertical line). Hopkins et al. (2007) compiled estimates of M_{cr} (their "M_{tr}") at different redshift. These are scaled to a Chabrier IMF and our cosmological parameters for comparison with our measurement. Defining M_{cr} as the stellar mass at which 50% of galaxies are optically blue or have a high specific star formation rate (calibrated using emission lines), they measure $M_{cr} \sim 1.6 - 3.8 \times 10^{10} M_\odot$ at $z \sim 0.4$, almost an order of magnitude lower than our estimate. This probably reflects our sensitivity to low levels of star formation in high mass galaxies. However, a definition of 50% morphologically late-type galaxies results in an estimate of $M_{cr} \sim 3 - 8 \times 10^{10} M_\odot$ at $z \sim 0.4$, much more compatible with our value within errors. This suggests that morphological selection is identifying more or less the same population as infrared selection. This is interesting, as it tells us that morphological transformation usually goes hand in hand with the final truncation of star formation in massive galaxies.

6. THE GROUP ENVIRONMENT

We will now examine how the fraction of InfraRed Excess galaxies depends upon the group environment by computing f(IRE) for group galaxies as a function of stellar mass. Groups were detected as overdensities in redshift space by applying a friends-of-friends algorithm to the CNOC2 redshift survey (Carlberg et al. 2001). Membership has been reassigned after inclusion of additional spectroscopy and application of the membership algorithm defined in Wilman et al. (2005)[8]. To ensure most group galaxies are not interlopers (i.e. nearby galaxies not bound to the group at the time of observation) the sample is limited to those within 500 kpc of the luminosity-weighted group centre. 500 kpc corresponds to the virial radius for a ~ 360 km s^{-1} group at z=0.4.

---

[7] CNOC2 consists of four patches spaced at intervals of ∼ 90° in RA, of which three are partially mapped by IRAC.

[8] The group aspect ratio, b, is set to 5.

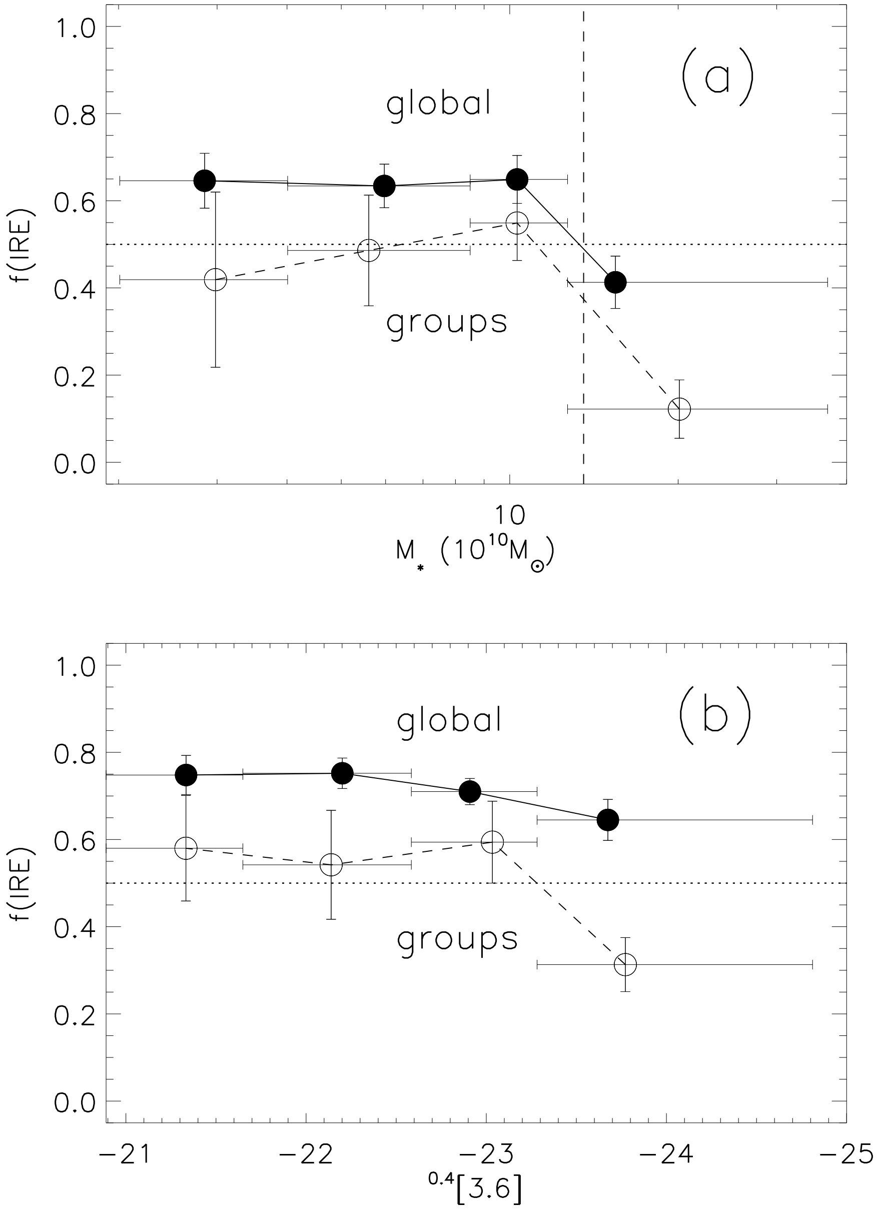

FIG. 5.— **(a)** The dependence of f(IRE) (the fraction of InfraRed Excess galaxies, defined by ${}^{0.4}[\mathrm{f}(8)/\mathrm{f}(3.6)] > 0.5$) for galaxies at $0.3 \leq z \leq 0.48$, divided into four bins of stellar mass (M_*). This is computed for the full (global) sample (solid line, solid points) and the group galaxy sample (dashed line, open points). Points are plotted at the median M_* of galaxies in each bin, and errors on f(IRE) are computed using a bootstrapping method (see text). There is a significant deficit of InfraRed Excess galaxies in groups, which nonetheless mirror the stellar mass dependence of the global population (f(IRE) decreases at high mass). A "*crossover mass*" (M_{cr}) at which f(IRE) = 0.5 (dotted horizontal line) is defined: For the global sample $\mathrm{M}_{\mathrm{cr}} \sim 1.3 \times 10^{11}\,\mathrm{M}_\odot$ (dashed vertical line). **(b)** As (a), except f(IRE) is plotted against ${}^{0.4}[3.6]$ luminosity for galaxies in a luminosity-limited sample.

Our decision to select group galaxies within a fixed radial aperture instead of a scaled aperture (e.g. the virial radius) is made because measurements of velocity dispersions are uncertain, and known to be heavily biased for systems with $\lesssim 30$ members (e.g. Zabludoff & Mulchaey 1998). 78/333 galaxies from the mass-selected sample match these group criteria. Of these 59% are in groups with measured velocity dispersions, $\sigma_{intr} < 360$ km s^{-1}; 80% are in groups with $\sigma_{intr} < 500$ km s^{-1}; and 6% are in the cluster g226 ($\sigma_{intr} \sim 850$ km s^{-1}).

The dashed line and open symbols in Figure 5**(a)** show how f(IRE) depends upon stellar mass for group galaxies only. Each bin contains 19 or 20 group galaxies by design, and appears to show a deficit of IRE galaxies with respect to the global population. This is not highly significant in individual mass bins, but is consistent at all masses. Thus we estimate the combined significance for the whole sample. In groups, the combined value of f(IRE) is 0.447. As the mass distribution of group galaxies is biased to high mass relative to the global sample, the global sample is resampled to match the group sample on mass. For each group galaxy, a random galaxy is selected from the nearest 10 galaxies in stellar mass (from the global sample, other than itself, and with no repeats). This resampling process is repeated 10000 times, each time computing f(IRE) for the matched sample. On only 56 out of 10000 occasions is f(IRE) ≤ 0.447. This corresponds to a 0.56% likelihood ($\sim 2.5\sigma$ from a one-tailed gaussian) that the low value of f(IRE) in groups arises by chance.

The lower value of f(IRE) in groups *independent of the stellar mass* indicates that activity in $\mathrm{M}_* \geq 2 \times 10^{10}\,\mathrm{M}_\odot$ galaxies is often suppressed by the group environment. As these groups are predominantly low velocity dispersion, often unvirialised systems, this means that massive galaxies are already affected by the low mass halo environment. The mechanism of suppression seems to be particularly active in the highest stellar mass bin ($\mathrm{M}_* \geq 1.27 \times 10^{11}\,\mathrm{M}_\odot$) where in groups $\mathrm{f(IRE)} = 0.12 \pm 0.07$. In this mass bin the group galaxies also dominate the passive global population: Out of a total of 43 galaxies (25 passive), 20 are in our group sample (17 passive). Hence the most massive galaxies seem to become passive in the group environment. This result is even more remarkable when it is considered that the group sample is incomplete due to incompleteness effects in the CNOC2 redshift survey, and so the global sample should include more group galaxies than have been identified.

It is prudent to repeat this exercise as a function of $^{0.4}[3.6]$ luminosity to ensure this result does not somehow depend upon our mass calibration. Figure 5**(b)** shows how f(IRE) depends upon $^{0.4}[3.6]$ luminosity for a luminosity-selected sample ($^{0.4}[3.6] \leq -20.89$). Luminosity selection allows an additional 180 $\mathrm{M}_* < 2 \times 10^{10}\,\mathrm{M}_\odot$ galaxies to make it into the sample with lower than maximum mass to light ratios. Effectively this means that the overall value of f(IRE) is higher for the luminosity-selected sample (0.735 ± 0.018) than for the mass-selected sample (0.621 ± 0.030). The trends mirror those seen as a function of mass with the exception that in the bin of highest luminosity the global f(IRE) is still quite high (0.645 ± 0.047). This is because IRE galaxies are more likely to be found in the high luminosity bin than in the high mass bin, due to their lower mass to light ratios. In groups the dominance of passive galaxies is so strong as to mitigate this effect.

7. DISCUSSION

MIR colour is a highly sensitive tracer of activity in galaxies. This has allowed us to separate truly passive galaxies (typically morphologically early-type) from galaxies with InfraRed Excess at 8μm (IRE galaxies). In this way we avoid confusion between galaxies with low but still ongoing star formation and those which have shutdown their star formation altogether (probably coincident with the morphological transformation). Other studies examine the evolution in fractions of highly star forming galaxies (LIRGs, ULIRGs etc: Bell et al. 2005; Le Floc'h et al. 2005; Hammer et al. 2005; Caputi et al. 2006; Daddi et al. 2007). These fractions decline steeply with cosmic time, with contributions from generally declining star formation rates in most galaxies, and complete suppression in some.

Our main result is that a strong and highly significant deficit in the fraction of InfraRed Excess galaxies, f(IRE), exists in optically selected, mostly low velocity dispersion groups at z∼0.4, and is *independent of stellar mass*. The suppression of infrared activity in low redshift Hickson Compact groups (Johnson et al. 2007) therefore extends to the "loose group" regime at z∼0.4.

Our group data indicate a dramatic drop in f(IRE) at stellar masses $\mathrm{M}_* \gtrsim 10^{11}\,\mathrm{M}_\odot$. This coincides with the stellar mass at which a galaxy's own halo usually exceeds $\mathrm{M}_{\mathrm{halo}} \sim 5 \times 10^{12}\,\mathrm{M}_\odot$, which is also the mass of the Local Group (Li & White 2007) and typical of the lower mass groups in our sample (McGee et al., submitted). Therefore galaxies with $\mathrm{M}_* \gtrsim 10^{11}\,\mathrm{M}_\odot$ are typically "central" galaxies in groups, which is why many of our most massive galaxies are members of known groups. *The low mass group environment suppresses star formation in both central massive galaxies and their satellites. The strongest effect is in the central galaxies.*

In this paper, we do not fully constrain the mechanism(s) responsible for suppressing activity in groups. For a discussion of the menagerie of possibilities we refer to Moran et al. (2007, and references therein). The ability to detect low levels of activity has important implications for the interpretation of passive spirals as identified purely from their [OII] emission (Poggianti et al. 1999; Balogh et al. 2002; Moran et al. 2006). Our strongest direct constraint on the mechanism(s) at work is that it (they) must be active in low mass group haloes. This probably excludes processes such as ram-pressure stripping which prefer much higher density environments (Gunn & Gott 1972; Quilis et al. 2000).

Relating the suppression of star formation to a halo mass threshold is theoretically attractive, as the physics of gas accretion and feedback are more likely to relate to the gravitationally bound material within the halo than to the stellar mass of the galaxy itself (e.g. Dekel & Birnboim 2006). For example, AGN feedback processes might be especially efficient in galaxies located inside group-sized haloes. Brightest Group Galaxies (BGGs) more frequently contain radio-loud AGN than similarly massive non-BGGs. This is likely to be related to the cooling of the hot Intra-Group Medium (IGM) onto the BGG, fuelling a radio-loud AGN (Best et al. 2007).

Our data alone is not sufficient to examine how the suppression of star formation within group-mass haloes contributes to the global population in a statistical manner. Incompleteness of the CNOC2 redshift survey and uncertainties in the construction of the group catalogue and galaxy membership inevitably leads to incompleteness of our group galaxy sample in a way which may depend upon galaxy stellar mass. To better estimate membership on a statistical basis, we use a simulated galaxy catalogue in which stellar mass and embedding halo mass can be directly evaluated for each galaxy at z=0.4. We choose the "mock" galaxy catalogue of Bower et al. (2006) which is based upon the Millenium Simulation, a simulated ΛCDM Universe with $500h_{100}^{-1}$ Mpc sides (Springel et al. 2005). These dark matter haloes are populated with mock galaxies using a semi-analytic technique. Only the positions (environment) and stellar masses of these galaxies are used. The mock galaxies are assumed to be in groups where they are located within haloes $\mathrm{M}_{\mathrm{halo}} \geq 5 \times 10^{12}\,\mathrm{M}_\odot$. Mock group galaxies are then assigned a probability that they are IRE galaxies consistent with the data: i.e. $\mathrm{f(IRE)} = 0.5$ for the $\mathrm{M}_* < 10^{11}\,\mathrm{M}_\odot$ galaxies and $\mathrm{f(IRE)} = 0.1$ for the $\mathrm{M}_* \geq 10^{11}\,\mathrm{M}_\odot$ galaxies (as seen in Figure 5**(a)**). Combined with the rest of the mock galaxy population ("field" galaxies), the dependence of f(IRE) upon stellar mass is compared to the CNOC2 global trend. By setting the fraction of IRE field galaxies to 0.9, regardless of their stellar mass, the global trend is well reproduced. This is demonstrated in Figure 6 **(a)** in which the observed global trend for CNOC2 galaxies (solid points) is extremely well matched by the model (solid line). That the fraction of field galaxies which need to be passive is low (0.1) *and independent of stellar mass* lends support to our hypothesis that the halo mass is more important than the stellar mass for the suppression of star formation in galaxies.

Figure 6 **(a)** also shows how f(IRE) depends upon stellar mass for the mock galaxy population evaluated at $z = 0$, 0.7, and 1. Remarkably, the model exhibits a *downsizing* behaviour, such that the crossover mass $\mathrm{M_{cr}}$ decreases at lower redshifts. This is shown in Figure 6 **(b)** with the CNOC2 datapoint at z=0.4. The only reason for this evolution is that the fraction of galaxies in groups increases, as a function of stellar mass, from $z = 1$ to $z = 0$. *Suppression of galaxy activity in groups, plus the gravitational growth of structure in the Universe, can explain downsizing trends in* $\mathrm{M_{cr}}$.

Also in Figure 6 **(b)** the crossover masses computed in different redshift bins by Bundy et al. (2006) are overplotted (reproduced from their Figure 9: $\mathrm{M_{cr}}$ is called the "*transition mass*" in that paper). These measurements are based on the DEEP2 redshift survey, and contribute to the compilation of Hopkins et al. (2007). $\mathrm{M_{cr}}$ is computed for 50% late-type morphologies, 50% galaxies blue in (U-B) colour, and 50% galaxies with [OII]-inferred SFR above $0.2\,\mathrm{M_\odot\,yr^{-1}}$. That more morphologically classified late-type galaxies are detected, resulting in a higher value of $\mathrm{M_{cr}}$, is fully in line with our estimate at z=0.4 using a sensitive MIR colour, well correlated with morphology. Whilst our simple model can qualitatively reproduce a downsizing scenario, comparison with Bundy et al. (2006) suggests that the redshift dependence is probably too shallow. With better constraints at different redshift, a model in which star formation is not immediately suppressed upon incorporation of a galaxy into a massive halo might serve to steepen this evolution.

8. CONCLUSIONS

From the CNOC2 redshift survey, we have constructed a mass-selected sample of galaxies with known spectroscopic redshifts $0.3 \leq z \leq 0.48$, and stellar masses $\mathrm{M_* \geq 2\times10^{10}\,M_\odot}$. Whilst the sample is not fully complete, the selection is well understood, and we correct for incompleteness using a simple weighting scheme. Within this sample, the fraction of galaxies with excess emission at 8μm is computed, which traces star formation or nuclear activity. For galaxies in this sample, the Mid InfraRed (MIR) colour $^{0.4}[\mathrm{f(8)/\,f(3.6)}]$ has been measured. This is the flux ratio of the 8μm to 3.6μm IRAC bands, k-corrected to a consistent rest-frame of a z=0.4 galaxy. Based upon this sample we have shown:

- **Infrared Passive Sequence:** Old stellar populations (such as found in passively evolving galaxies in which star formation has been suppressed) exhibit very predictable colours in the $\sim 2-7\mu$m spectral region (rest-frame), tracing the stellar atmospheres of giant M-stars. This produces a tight **Infrared Passive Sequence (IPS)** in the $^{0.4}[\mathrm{f(8)/\,f(3.6)}]$ colour. The IPS does not suffer from the optical red sequence degeneracy between dusty red galaxies and passive red galaxies. The mean IPS colour ($^{0.4}[\mathrm{f(8)/\,f(3.6)}] = 0.34$ at $\mathrm{M_* > 6\times10^{10}\,M_\odot}$) is consistent with an old stellar population, and the tight scatter ($0.03-0.05$ at high mass) is consistent with photometric errors. This leaves little room for large variations in metallicity, or additional contributions at $\sim 6\mu$m from circumstellar or diffuse dust.

- **MIR Colour Bimodality:** The $^{0.4}[\mathrm{f(8)/\,f(3.6)}]$ distribution is bimodal, consisting of the IPS and a population of galaxies with significant excess emission at 8μm (InfraRed-Excess Galaxies). These two populations can be divided at $^{0.4}[\mathrm{f(8)/\,f(3.6)}] = 0.5$.

- **Morphologies and infrared emission:** 15 out of 17 morphologically classified early-type (elliptical or S0) galaxies have $^{0.4}[\mathrm{f(8)/\,f(3.6)}]$ colours consistent with the IPS, whilst no classified late-type galaxy has $^{0.4}[\mathrm{f(8)/\,f(3.6)}] < 0.5$. This is consistent with known correlations at low redshift between morphology and MIR colours (e.g. Pahre et al. 2004a; Li et al. 2007).

- **Tracing low level activity in the MIR:** There is a strong correlation between $^{0.4}[\mathrm{f(8)/\,f(3.6)}]$ and EW[OII]. However, our division at $^{0.4}[\mathrm{f(8)/\,f(3.6)}] = 0.5$ corresponds to a division at EW[OII]= 2.1Å for the median galaxy. This is below the [OII] detection limit of most intermediate to high redshift surveys. This shows that MIR diagnostics trace low levels of activity at $z \sim 0.4$. Consequently, dividing at $^{0.4}[\mathrm{f(8)/\,f(3.6)}] = 0.5$ selects a high fraction of InfraRed-Excess (IRE) galaxies, f(IRE), and the crossover mass at which f(IRE) = 0.5, $\mathrm{M_{cr} \sim 1.3\times10^{11}\,M_\odot}$, is also high with respect to optical studies.

- **Consequences for selection of passive spirals:** There exist spiral galaxies in our sample with undetected [OII] emission but significant MIR excess emission ($^{0.4}[\mathrm{f(8)/\,f(3.6)}] > 0.5$). Thus, selection of passive spirals based upon a simple EW[OII] division (e.g. Poggianti et al. 1999; Balogh et al. 2002; Moran et al. 2006) will suffer contamination by dusty, low level star formation, mostly early-type spirals.

- **Strong suppression of activity for massive galaxies in low mass groups:** In the $z \sim 0.4$ optically-selected group environment there is a strong and robust (2.5σ) deficit in f(IRE) compared with global values, *independent of stellar mass*. This is true across our range in stellar mass $\mathrm{M_* \geq 2\times10^{10}\,M_\odot}$, but the suppression appears to be particularly strong at high mass $\mathrm{M_* \gtrsim 10^{11}\,M_\odot}$, where the fraction of active group galaxies falls to f(IRE) $= 0.12 \pm 0.07$.

- **Suppression in groups can drive the stellar mass dependence, and structure growth can drive downsizing:** The global dependence of f(IRE) on stellar mass at z=0.4 can be accurately reproduced by a simple model in which suppression mainly occurs in groups, and is particularly strong

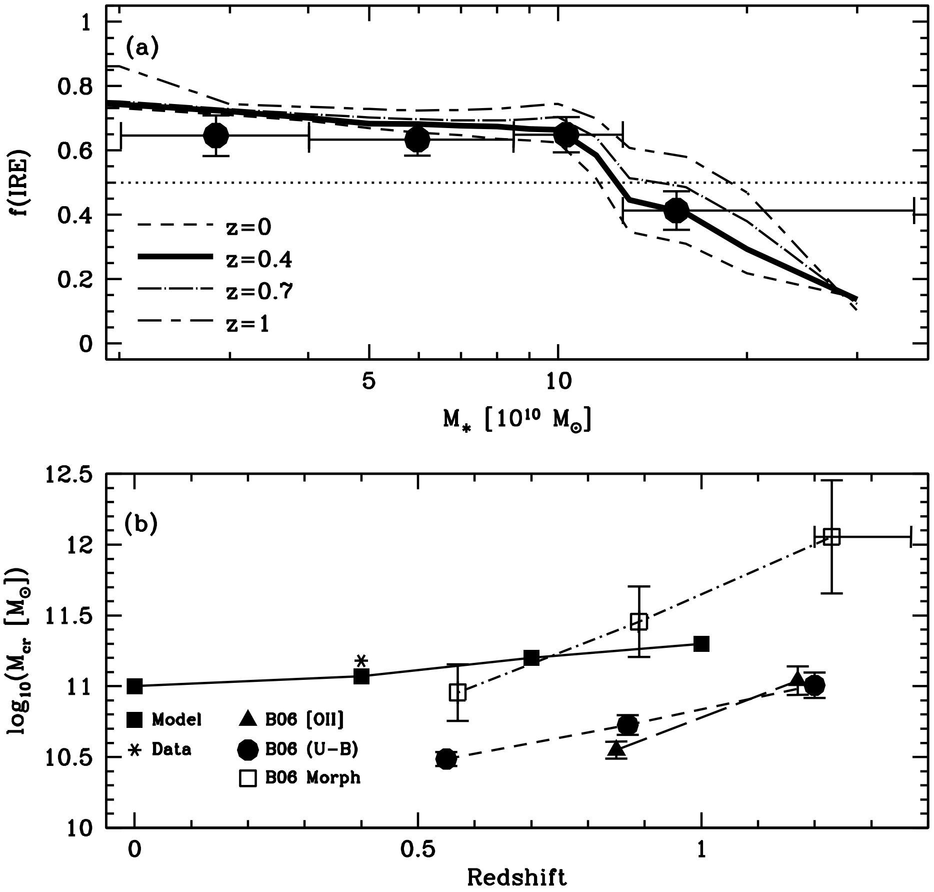

FIG. 6.— **(a)** The dependence of f(IRE) on stellar mass M_* for the global population of $0.3 \leq z \leq 0.48$ CNOC2 galaxies compared with our simple model predictions at $z = 0.4$. The model predictions are also computed at $z = 0$, 0.7, and 1. Galaxies in haloes with $M_{\rm halo} \geq 5 \times 10^{12}\,M_\odot$ are considered to be in groups. The stellar mass dependence can be reproduced by a model in which suppression of galaxy activity is driven primarily by the group environment. **(b)** Evolution of the crossover mass $M_{\rm cr}$ (where 50% of all galaxies are active, computed in various ways). Our data point ($M_{\rm cr}$ at z=0.4 computed using f(IRE) = 0.5 in CNOC2) is compared with the model predictions at $z = 0, 0.4, 0.7$, and 1, and DEEP2 crossover masses computed in different redshift bins by Bundy et al. (2006, B06) for 50% late-type morphologies, 50% galaxies blue in (U-B) colour, and 50% [OII]-inferred SFR above $0.2\,M_\odot\,{\rm yr}^{-1}$. Our simple model can qualitatively reproduce a downsizing scenario, although the redshift dependence is shallower than observed by B06.

for $M_* \geq 10^{11}\,M_\odot$ group galaxies. Furthermore, structure growth in the Universe drives more galaxies into group-sized haloes with cosmic time. This automatically leads to a *downsizing* phenomenon in the global population, in which the crossover mass $M_{\rm cr}$ evolves to lower masses at lower redshift.

We thank the anonymous referee for substantial help with improving the manuscript. We would like to thank the CNOC2 team for allowing us access to their unpublished data, and Dr. Eckhard Sturm for providing us with the calibrated ISO-SWS spectrum of M82 in ASCII format. This work is based on observations made with the Spitzer Space Telescope, which is operated by the Jet Propulsion Laboratory, California Institute of Technology under a contract with NASA. It is also based on observations made with the NASA/ESA Hubble Space Telescope, at the Space Telescope Science Institute, which is operated by the Association of Universities for Research in Astronomy, Inc., under NASA contract NAS 5-26555. These observations are associated with program 9895. DW and DP are supported by the Max Planck Society.

REFERENCES

Aaronson, M., Huchra, J., & Mould, J. 1979, ApJ, 229, 1
Aitken, D. K., Roche, P. F., Allen, M. C., & Phillips, M. M. 1982, MNRAS, 199, 31P
Baldry, I. K., Balogh, M. L., Bower, R. G., Glazebrook, K., Nichol, R. C., Bamford, S. P., & Budavari, T. 2006, MNRAS, 373, 469
Balogh, M., Bower, R. G., Smail, I., Ziegler, B. L., Davies, R. L., Gaztelu, A., & Fritz, A. 2002, MNRAS, 337, 256
Balogh, M., Eke, V., Miller, C., Lewis, I., Bower, R., Couch, W., Nichol, R., Bland-Hawthorn, J., Baldry, I. K., Baugh, C., Bridges, T., Cannon, R., Cole, S., Colless, M., Collins, C., Cross, N., Dalton, G., de Propris, R., Driver, S. P., Efstathiou, G., Ellis, R. S., Frenk, C. S., Glazebrook, K., Gomez, P., Gray, A., Hawkins, E., Jackson, C., Lahav, O., Lumsden, S., Maddox, S., Madgwick, D., Norberg, P., Peacock, J. A., Percival, W., Peterson, B. A., Sutherland, W., & Taylor, K. 2004, MNRAS, 348, 1355
Balogh, M. L., Wilman, D., Henderson, R. D. E., Bower, R. G., Gilbank, D., Whitaker, R., Morris, S. L., Hau, G., Mulchaey, J. S., Oemler, A., & Carlberg, R. G. 2007, MNRAS, 374, 1169
Bell, E. F. & de Jong, R. S. 2001, ApJ, 550, 212

Bell, E. F., Papovich, C., Wolf, C., Le Floc'h, E., Caldwell, J. A. R., Barden, M., Egami, E., McIntosh, D. H., Meisenheimer, K., Pérez-González, P. G., Rieke, G. H., Rieke, M. J., Rigby, J. R., & Rix, H.-W. 2005, ApJ, 625, 23

Bender, R., Saglia, R. P., Ziegler, B., Belloni, P., Greggio, L., Hopp, U., & Bruzual, G. 1998, ApJ, 493, 529

Benson, A. J., Ellis, R. S., & Menanteau, F. 2002, MNRAS, 336, 564

Berta, S., Lonsdale, C. J., Siana, B., Farrah, D., Smith, H. E., Polletta, M. C., Franceschini, A., Fritz, J., Perez-Fournon, I., Rowan-Robinson, M., Shupe, D., & Surace, J. 2007, A&A, 467, 565

Bertin, E. & Arnouts, S. 1996, A&AS, 117, 393

Best, P. N., von der Linden, A., Kauffmann, G., Heckman, T. M., & Kaiser, C. R. 2007, MNRAS, 379, 894

Blanton, M. R. & Roweis, S. 2007, AJ, 133, 734

Boselli, A., Lequeux, J., & Gavazzi, G. 2004, A&A, 428, 409

Boselli, A., Lequeux, J., Sauvage, M., Boulade, O., Boulanger, F., Cesarsky, D., Dupraz, C., Madden, S., Viallefond, F., & Vigroux, L. 1998, A&A, 335, 53

Boselli, A., Sauvage, M., Lequeux, J., Donati, A., & Gavazzi, G. 2003, A&A, 406, 867

Bower, R. G., Benson, A. J., Malbon, R., Helly, J. C., Frenk, C. S., Baugh, C. M., Cole, S., & Lacey, C. G. 2006, MNRAS, 370, 645

Bower, R. G., Lucey, J. R., & Ellis, R. S. 1992, MNRAS, 254, 601

Bressan, A., Panuzzo, P., Silva, L., Buson, L., Clemens, M., Granato, G. L., Rampazzo, R., Valdes, J. R., & Vega, O. 2007, in Astronomical Society of the Pacific Conference Series, Vol. 374, Astronomical Society of the Pacific Conference Series, ed. A. Vallenari, R. Tantalo, L. Portinari, & A. Moretti, 333–+

Brinchmann, J., Charlot, S., White, S. D. M., Tremonti, C., Kauffmann, G., Heckman, T., & Brinkmann, J. 2004, MNRAS, 351, 1151

Bruzual, G. & Charlot, S. 2003, MNRAS, 344, 1000

Bundy, K., Ellis, R. S., Conselice, C. J., Taylor, J. E., Cooper, M. C., Willmer, C. N. A., Weiner, B. J., Coil, A. L., Noeske, K. G., & Eisenhardt, P. R. M. 2006, ApJ, 651, 120

Calura, F., Pipino, A., & Matteucci, F. 2007, ArXiv e-prints, 706

Calzetti, D., Kennicutt, R. C., Engelbracht, C. W., Leitherer, C., Draine, B. T., Kewley, L., Moustakas, J., Sosey, M., Dale, D. A., Gordon, K. D., Helou, G. X., Hollenbach, D. J., Armus, L., Bendo, G., Bot, C., Buckalew, B., Jarrett, T., Li, A., Meyer, M., Murphy, E. J., Prescott, M., Regan, M. W., Rieke, G. H., Roussel, H., Sheth, K., Smith, J. D. T., Thornley, M. D., & Walter, F. 2007, ApJ, 666, 870

Caputi, K. I., Dole, H., Lagache, G., McLure, R. J., Dunlop, J. S., Puget, J.-L., Le Floc'h, E., & Pérez-González, P. G. 2006, A&A, 454, 143

Carlberg, R. G., Yee, H. K. C., Morris, S. L., Lin, H., Hall, P. B., Patton, D. R., Sawicki, M., & Shepherd, C. W. 2001, ApJ, 552, 427

Chabrier, G. 2003, PASP, 115, 763

Cimatti, A., Daddi, E., Mignoli, M., Pozzetti, L., Renzini, A., Zamorani, G., Broadhurst, T., Fontana, A., Saracco, P., Poli, F., Cristiani, S., D'Odorico, S., Giallongo, E., Gilmozzi, R., & Menci, N. 2002, A&A, 381, L68

Cimatti, A., Daddi, E., Renzini, A., Cassata, P., Vanzella, E., Pozzetti, L., Cristiani, S., Fontana, A., Rodighiero, G., Mignoli, M., & Zamorani, G. 2004, Nature, 430, 184

Cowie, L. L., Songaila, A., & Barger, A. J. 1999, AJ, 118, 603

Croton, D. J., Springel, V., White, S. D. M., De Lucia, G., Frenk, C. S., Gao, L., Jenkins, A., Kauffmann, G., Navarro, J. F., & Yoshida, N. 2006, MNRAS, 365, 11

Daddi, E., Dickinson, M., Morrison, G., Chary, R., Cimatti, A., Elbaz, D., Frayer, D., Renzini, A., Pope, A., Alexander, D. M., Bauer, F. E., Giavalisco, M., Huynh, M., Kurk, J., & Mignoli, M. 2007, ApJ, 670, 156

Dale, D. A., Silbermann, N. A., Helou, G., Valjavec, E., Malhotra, S., Beichman, C. A., Brauher, J., Contursi, A., Dinerstein, H. L., Hollenbach, D. J., Hunter, D. A., Kolhatkar, S., Lo, K.-Y., Lord, S. D., Lu, N. Y., Rubin, R. H., Stacey, G. J., Thronson, Jr., H. A., Werner, M. W., & Corwin, Jr., H. G. 2000, AJ, 120, 583

Davoodi, P., Pozzi, F., Oliver, S., Polletta, M., Afonso-Luis, A., Farrah, D., Hatziminaoglou, E., Rodighiero, G., Berta, S., Waddington, I., Lonsdale, C., Rowan-Robinson, M., Shupe, D. L., Evans, T., Fang, F., Smith, H. E., & Surace, J. 2006, MNRAS, 371, 1113

De Lucia, G., Springel, V., White, S. D. M., Croton, D., & Kauffmann, G. 2006, MNRAS, 366, 499

Dekel, A. & Birnboim, Y. 2006, MNRAS, 368, 2

Desert, F.-X., Boulanger, F., & Puget, J. L. 1990, A&A, 237, 215

Draine, B. T., Dale, D. A., Bendo, G., Gordon, K. D., Smith, J. D. T., Armus, L., Engelbracht, C. W., Helou, G., Kennicutt, Jr., R. C., Li, A., Roussel, H., Walter, F., Calzetti, D., Moustakas, J., Murphy, E. J., Rieke, G. H., Bot, C., Hollenbach, D. J., Sheth, K., & Teplitz, H. I. 2007, ApJ, 663, 866

Duc, P.-A., Poggianti, B. M., Fadda, D., Elbaz, D., Flores, H., Chanial, P., Franceschini, A., Moorwood, A., & Cesarsky, C. 2002, A&A, 382, 60

Eggen, O. J., Lynden-Bell, D., & Sandage, A. R. 1962, ApJ, 136, 748

Engelbracht, C. W., Gordon, K. D., Rieke, G. H., Werner, M. W., Dale, D. A., & Latter, W. B. 2005, ApJ, 628, L29

Fazio, G. G., Hora, J. L., Allen, L. E., Ashby, M. L. N., Barmby, P., Deutsch, L. K., Huang, J.-S., Kleiner, S., Marengo, M., Megeath, S. T., Melnick, G. J., Pahre, M. A., Patten, B. M., Polizotti, J., Smith, H. A., Taylor, R. S., Wang, Z., Willner, S. P., Hoffmann, W. F., Pipher, J. L., Forrest, W. J., McMurty, C. W., McCreight, C. R., McKelvey, M. E., McMurray, R. E., Koch, D. G., Moseley, S. H., Arendt, R. G., Mentzell, J. E., Marx, C. T., Losch, P., Mayman, P., Eichhorn, W., Krebs, D., Jhabvala, M., Gezari, D. Y., Fixsen, D. J., Flores, J., Shakoorzadeh, K., Jungo, R., Hakun, C., Workman, L., Karpati, G., Kichak, R., Whitley, R., Mann, S., Tollestrup, E. V., Eisenhardt, P., Stern, D., Gorjian, V., Bhattacharya, B., Carey, S., Nelson, B. O., Glaccum, W. J., Lacy, M., Lowrance, P. J., Laine, S., Reach, W. T., Stauffer, J. A., Surace, J. A., Wilson, G., Wright, E. L., Hoffman, A., Domingo, G., & Cohen, M. 2004, ApJS, 154, 10

Fioc, M. & Rocca-Volmerange, B. 1997, A&A, 326, 950

Fisher, D. B. 2006, ApJ, 642, L17

Förster Schreiber, N. M., Genzel, R., Lutz, D., Kunze, D., & Sternberg, A. 2001, ApJ, 552, 544

Förster Schreiber, N. M., Roussel, H., Sauvage, M., & Charmandaris, V. 2004, A&A, 419, 501

Gómez, P. L., Nichol, R. C., Miller, C. J., Balogh, M. L., Goto, T., Zabludoff, A. I., Romer, A. K., Bernardi, M., Sheth, R., Hopkins, A. M., Castander, F. J., Connolly, A. J., Schneider, D. P., Brinkmann, J., Lamb, D. Q., SubbaRao, M., & York, D. G. 2003, ApJ, 584, 210

Genzel, R. & Cesarsky, C. J. 2000, ARA&A, 38, 761

Genzel, R., Lutz, D., Sturm, E., Egami, E., Kunze, D., Moorwood, A. F. M., Rigopoulou, D., Spoon, H. W. W., Sternberg, A., Tacconi-Garman, L. E., Tacconi, L., & Thatte, N. 1998, ApJ, 498, 579

Gerke, B. F., Newman, J. A., Faber, S. M., Cooper, M. C., Croton, D. J., Davis, M., Willmer, C. N. A., Yan, R., Coil, A. L., Guhathakurta, P., Koo, D. C., & Weiner, B. J. 2007, MNRAS, 376, 1425

Giovanelli, R., Haynes, M. P., Salzer, J. J., Wegner, G., da Costa, L. N., & Freudling, W. 1995, AJ, 110, 1059

Gunn, J. E. & Gott, J. R. I. 1972, ApJ, 176, 1

Haines, C. P., Gargiulo, A., & Merluzzi, P. 2007, ArXiv e-prints, 707

Hammer, F., Flores, H., Elbaz, D., Zheng, X. Z., Liang, Y. C., & Cesarsky, C. 2005, A&A, 430, 115

Hopkins, A. M. 2004, ApJ, 615, 209

Hopkins, P. F., Bundy, K., Hernquist, L., & Ellis, R. S. 2007, ApJ, 659, 976

Huang, J.-S., Ashby, M. L. N., Barmby, P., Brodwin, M., Brown, M. J. I., Caldwell, N., Cool, R. J., Eisenhardt, P., Eisenstein, D., Fazio, G. G., Le Floc'h, E., Green, P., Kochanek, C. S., Lu, N., Pahre, M. A., Rigopoulou, D., Rosenberg, J. L., Smith, H. A., Wang, Z., Willmer, C. N. A., & Willner, S. P. 2007, ApJ, 664, 840

Johnson, K. E., Hibbard, J. E., Gallagher, S. C., Charlton, J. C., Hornschemeier, A. E., Jarrett, T. H., & Reines, A. E. 2007, AJ, 134, 1522

Kauffmann, G., Heckman, T. M., White, S. D. M., Charlot, S., Tremonti, C., Peng, E. W., Seibert, M., Brinkmann, J., Nichol, R. C., SubbaRao, M., & York, D. 2003, MNRAS, 341, 54

Laurent, O., Mirabel, I. F., Charmandaris, V., Gallais, P., Madden, S. C., Sauvage, M., Vigroux, L., & Cesarsky, C. 2000, A&A, 359, 887

Le Floc'h, E., Papovich, C., Dole, H., Bell, E. F., Lagache, G., Rieke, G. H., Egami, E., Pérez-González, P. G., Alonso-Herrero, A., Rieke, M. J., Blaylock, M., Engelbracht, C. W., Gordon, K. D., Hines, D. C., Misselt, K. A., Morrison, J. E., & Mould, J. 2005, ApJ, 632, 169

Leger, A. & Puget, J. L. 1984, A&A, 137, L5

Lewis, I., Balogh, M., De Propris, R., Couch, W., Bower, R., Offer, A., Bland-Hawthorn, J., Baldry, I. K., Baugh, C., Bridges, T., Cannon, R., Cole, S., Colless, M., Collins, C., Cross, N., Dalton, G., Driver, S. P., Efstathiou, G., Ellis, R. S., Frenk, C. S., Glazebrook, K., Hawkins, E., Jackson, C., Lahav, O., Lumsden, S., Maddox, S., Madgwick, D., Norberg, P., Peacock, J. A., Percival, W., Peterson, B. A., Sutherland, W., & Taylor, K. 2002, MNRAS, 334, 673

Li, H.-N., Wu, H., Cao, C., & Zhu, Y.-N. 2007, AJ, 134, 1315

Li, Y.-S. & White, S. D. M. 2007, ArXiv e-prints, 710

Lilly, S. J., Le Fevre, O., Hammer, F., & Crampton, D. 1996, ApJL, 460, L1+

Lotz, J. M., Davis, M., Faber, S. M., Guhathakurta, P., Gwyn, S., Huang, J., Koo, D. C., Le Floc'h, E., Lin, L., Newman, J., Noeske, K., Papovich, C., Willmer, C. N. A., Coil, A., Conselice, C. J., Cooper, M., Hopkins, A. M., Metevier, A., Primack, J., Rieke, G., & Weiner, B. J. 2008, ApJ, 672, 177

Madau, P., Pozzetti, L., & Dickinson, M. 1998, ApJ, 498, 106

Masters, K. L., Giovanelli, R., & Haynes, M. P. 2003, AJ, 126, 158

Moran, S. M., Ellis, R. S., Treu, T., Salim, S., Rich, R. M., Smith, G. P., & Kneib, J.-P. 2006, ApJ, 641, L97

Moran, S. M., Ellis, R. S., Treu, T., Smith, G. P., Rich, R. M., & Smail, I. 2007, ApJ, 671, 1503

Pahre, M. A., Ashby, M. L. N., Fazio, G. G., & Willner, S. P. 2004a, ApJS, 154, 235

—. 2004b, ApJS, 154, 229

Pannella, M., Hopp, U., Saglia, R. P., Bender, R., Drory, N., Salvato, M., Gabasch, A., & Feulner, G. 2006, ApJ, 639, L1

Panter, B., Heavens, A. F., & Jimenez, R. 2003, MNRAS, 343, 1145

Papovich, C., Moustakas, L. A., Dickinson, M., Le Floc'h, E., Rieke, G. H., Daddi, E., Alexander, D. M., Bauer, F., Brandt, W. N., Dahlen, T., Egami, E., Eisenhardt, P., Elbaz, D., Ferguson, H. C., Giavalisco, M., Lucas, R. A., Mobasher, B., Pérez-González, P. G., Stutz, A., Rieke, M. J., & Yan, H. 2006, ApJ, 640, 92

Peeters, E., Spoon, H. W. W., & Tielens, A. G. G. M. 2004, ApJ, 613, 986

Pérez-González, P. G., Kennicutt, Jr., R. C., Gordon, K. D., Misselt, K. A., Gil de Paz, A., Engelbracht, C. W., Rieke, G. H., Bendo, G. J., Bianchi, L., Boissier, S., Calzetti, D., Dale, D. A., Draine, B. T., Jarrett, T. H., Hollenbach, D., & Prescott, M. K. M. 2006, ApJ, 648, 987

Phillips, M. M., Aitken, D. K., & Roche, P. F. 1984, MNRAS, 207, 25

Pierini, D., Maraston, C., Bender, R., & Witt, A. N. 2004, MNRAS, 347, 1

Piovan, L., Tantalo, R., & Chiosi, C. 2003, A&A, 408, 559

Poggianti, B. M., Bridges, T. J., Komiyama, Y., Yagi, M., Carter, D., Mobasher, B., Okamura, S., & Kashikawa, N. 2004, ApJ, 601, 197

Poggianti, B. M., Smail, I., Dressler, A., Couch, W. J., Barger, A. J., Butcher, H., Ellis, R. S., & Oemler, A. J. 1999, ApJ, 518, 576

Popescu, C. C., Misiriotis, A., Kylafis, N. D., Tuffs, R. J., & Fischera, J. 2000, A&A, 362, 138

Postman, M. & Geller, M. J. 1984, ApJ, 281, 95

Quilis, V., Moore, B., & Bower, R. 2000, Science, 288, 1617

Rieke, G. H., Young, E. T., Engelbracht, C. W., Kelly, D. M., Low, F. J., Haller, E. E., Beeman, J. W., Gordon, K. D., Stansberry, J. A., Misselt, K. A., Cadien, J., Morrison, J. E., Rivlis, G., Latter, W. B., Noriega-Crespo, A., Padgett, D. L., Stapelfeldt, K. R., Hines, D. C., Egami, E., Muzerolle, J., Alonso-Herrero, A., Blaylock, M., Dole, H., Hinz, J. L., Le Floc'h, E., Papovich, C., Pérez-González, P. G., Smith, P. S., Su, K. Y. L., Bennett, L., Frayer, D. T., Henderson, D., Lu, N., Masci, F., Pesenson, M., Rebull, L., Rho, J., Keene, J., Stolovy, S., Wachter, S., Wheaton, W., Werner, M. W., & Richards, P. L. 2004, ApJS, 154, 25

Rix, H.-W. & Rieke, M. J. 1993, ApJ, 418, 123

Roche, P. F., Aitken, D. K., Smith, C. H., & Ward, M. J. 1991, MNRAS, 248, 606

Roche, P. F., Whitmore, B., Aitken, D. K., & Phillips, M. M. 1984, MNRAS, 207, 35

Roussel, H., Sauvage, M., Vigroux, L., & Bosma, A. 2001, A&A, 372, 427

Rowan-Robinson, M., Babbedge, T., Surace, J., Shupe, D., Fang, F., Lonsdale, C., Smith, G., Polletta, M., Siana, B., Gonzalez-Solares, E., Xu, K., Owen, F., Davoodi, P., Dole, H., Domingue, D., Efstathiou, A., Farrah, D., Fox, M., Franceschini, A., Frayer, D., Hatziminaoglou, E., Masci, F., Morrison, G., Nandra, K., Oliver, S., Onyett, N., Padgett, D., Perez-Fournon, I., Serjeant, S., Stacey, G., & Vaccari, M. 2005, AJ, 129, 1183

Salim, S., Charlot, S., Rich, R. M., Kauffmann, G., Heckman, T. M., Barlow, T. A., Bianchi, L., Byun, Y.-I., Donas, J., Forster, K., Friedman, P. G., Jelinsky, P. N., Lee, Y.-W., Madore, B. F., Malina, R. F., Martin, D. C., Milliard, B., Morrissey, P., Neff, S. G., Schiminovich, D., Seibert, M., Siegmund, O. H. W., Small, T., Szalay, A. S., Welsh, B. Y., & Wyder, T. K. 2005, ApJ, 619, L39

Salpeter, E. E. 1955, ApJ, 121, 161

Shi, Y., Ogle, P., Rieke, G. H., Antonucci, R., Hines, D. C., Smith, P. S., Low, F. J., Bouwman, J., & Willmer, C. 2007, ApJ, 669, 841

Springel, V., White, S. D. M., Jenkins, A., Frenk, C. S., Yoshida, N., Gao, L., Navarro, J., Thacker, R., Croton, D., Helly, J., Peacock, J. A., Cole, S., Thomas, P., Couchman, H., Evrard, A., Colberg, J., & Pearce, F. 2005, Nature, 435, 629

Temi, P., Brighenti, F., & Mathews, W. G. 2008, ApJ, 672, 244

Thomas, D., Maraston, C., Bender, R., & Mendes de Oliveira, C. 2005, ApJ, 621, 673

Tuffs, R. J., Popescu, C. C., Völk, H. J., Kylafis, N. D., & Dopita, M. A. 2004, A&A, 419, 821

Wang, B. & Heckman, T. M. 1996, ApJ, 457, 645

Weiner, B. J., Papovich, C., Bundy, K., Conselice, C. J., Cooper, M. C., Ellis, R. S., Ivison, R. J., Noeske, K. G., Phillips, A. C., & Yan, R. 2007, ApJ, 660, L39

Weinmann, S. M., van den Bosch, F. C., Yang, X., & Mo, H. J. 2006, MNRAS, 366, 2

Wilman, D. J., Balogh, M. L., Bower, R. G., Mulchaey, J. S., Oemler, A., Carlberg, R. G., Morris, S. L., & Whitaker, R. J. 2005, MNRAS, 358, 71

Wolf, C., Gray, M. E., & Meisenheimer, K. 2005, A&A, 443, 435

Yamada, T., Kodama, T., Akiyama, M., Furusawa, H., Iwata, I., Kajisawa, M., Iye, M., Ouchi, M., Sekiguchi, K., Shimasaku, K., Simpson, C., Tanaka, I., & Yoshida, M. 2005, ApJ, 634, 861

Yan, R., Newman, J. A., Faber, S. M., Konidaris, N., Koo, D., & Davis, M. 2006, ApJ, 648, 281

Yee, H. K. C., Morris, S. L., Lin, H., Carlberg, R. G., Hall, P. B., Sawicki, M., Patton, D. R., Wirth, G. D., Ellingson, E., & Shepherd, C. W. 2000, ApJS, 129, 475

Zabludoff, A. I. & Mulchaey, J. S. 1998, ApJ, 496, 39

Zheng, X. Z., Dole, H., Bell, E. F., Le Floc'h, E., Rieke, G. H., Rix, H.-W., & Schiminovich, D. 2007, ApJ, 670, 301